UC Berkeley
UC Berkeley Electronic Theses and Dissertations

**Title**
Mechanobiological Regulation of Glioblastoma Initiation and Invasion

**Permalink**
https://escholarship.org/uc/item/2h64b96m

**Author**
Wong, Sophie Y.

**Publication Date**
2015

Peer reviewed|Thesis/dissertation

eScholarship.org Powered by the California Digital Library
University of California

**Mechanobiological Regulation of Glioblastoma Initiation and Invasion**

by

Sophie Yanlok Wong

A dissertation submitted in partial satisfaction of the

requirements for the degree of

Joint Doctor of Philosophy

with University of California, San Francisco

in

Bioengineering

in the

Graduate Division

of the

University of California, Berkeley

Committee in charge:

Professor Sanjay Kumar, Chair
Professor Tejal A. Desai
Professor Daniela Kaufer

Spring 2015

Mechanobiological Regulation of Glioblastoma Initiation and Invasion

© 2015

By Sophie Yanlok Wong

Abstract

Mechanobiological Regulation of Glioblastoma Initiation and Invasion

by

Sophie Yanlok Wong

Joint Doctor of Philosophy in Bioengineering
with University of California, San Francisco

University of California, Berkeley

Professor Sanjay Kumar, Chair

Glioblastoma remains elusive to treat due to the diffuse infiltration of single tumor cells into the surrounding tissue. Current standard therapies - surgery, radiation, chemotherapy - have been ineffective at significantly increasing survival time. Although many studies have focused on factors that affect glioma growth and invasion, it is still unclear how and why this disease is so aggressive. Promising chemotherapeutic drugs have failed in clinical trials even though specific targets were identified. The existence of tumor-initiating cells (TICs), a subpopulation within primary tumors, could explain how the heterogeneous makeup of the bulk tumor leads to quick adaptability to resist surrounding cues that limit migration and growth. The work presented in this dissertation has approached this problem from a biophysical perspective, demonstrating that the extracellular matrix (ECM) can serve as a regulator of TIC invasion and initiation both *in vitro* and *in vivo*.

We first characterized TIC migration and growth on 2D ECMs and found that they were able to migrate readily even on soft ECMs. Noting that cellular contractility is important for cells to sense environmental cues in the surrounding tissue, we manipulated the TICs with upregulation of myosin activators. Thus, we were able to rescue mechanosensing in the TICs and found that migration of the CA RhoA TICs was limited on soft ECMs. We then used 3D invasion assays to confirm that high contractility in TICs limits invasion and migration in 3D as well. Lastly, we implanted CA RhoA TICs in orthotopic mouse models and found that increased cellular contractility limits tumor occupancy and significantly increases survival time.

*This dissertation is dedicated to my loving husband, Donald*

*for his enthusiastic support of my dreams,*

*for always nurturing me with delicious meals,*

*for driving me to and from lab regardless of the time of day or night,*

*for inspiring me to pursue my passions in life.*

# Table of Contents

**Acknowledgements**.....v

**Chapter 1: Introduction to matrix regulation of tumor-initiating cells**.....1

1.1 Abstract.....2

1.2 Introduction.....2

1.3 Significance of TICs.....3

1.4 Identification and isolation of TICs.....4

1.5 Role of extracellular matrix and mechanical signals in regulating TIC function.....5

1.6 Propagation of TICs in ECM-adherent cultures.....6

1.7 Mechanisms of mechanotransduction .....7

1.8 Discussion .....8

**Chapter 2: Constitutive activation of Myosin-dependent contractility sensitizes glioma tumor-initiating cells to mechanical inputs and reduces tissue invasion**.....10

2.1 Abstract.....11

2.2 Introduction.....11

2.3 Materials and Methods.....12

2.3.1 Tumor sample and primary cell culture.....12

2.3.2 Continuous cell line culture.....13

2.3.3 Identification of slow-cycling population using CFSE and flow cytometry.....13

2.3.4 Differentiation of brain tumor-initiating cells.....13

2.3.5 Synthesis and functionalization of extracellular matrices.....14

2.3.6 Phase and epifluorescence imaging and immunofluorescence staining.....14

2.3.7 Measurement and analysis of cell motility.....14

2.3.8 Measurement of cell proliferation.....14

2.3.9 Constitutively active cell lines.....15

2.3.10 Western blot analysis.....15

2.3.11 Atomic force microscopy (AFM) protocol.....15

2.3.12 Sphere forming frequency assay and sphere size measurement.....15

2.3.13 Pharmacologic inhibition of cell motility.....16

2.3.14 Live/dead assay.....16

2.3.15 Mass spectroscopy quantification of NM II isoform expression.....16

2.3.16 Collagen invasion assay.....16

2.3.17 Transwell migration assay.....16

2.3.18 Xenotransplantation of human primary brain tumor-initiating cells into mice .....16

2.3.19 Immunohistochemistry.....17

2.3.20 Tumor occupancy measurement.....17

2.3.21 Statistical analysis.....17

2.4 Results.....17

2.4.1 Tumor-initiating population is maintained on soft and stiff ECMs.....17

2.4.2 Tumor-initiating cells can spread, migrate, and proliferate on soft and stiff ECMs.....19

2.4.3 Myosin II-dependent contractility restricts rigidity-dependent spreading, motility, and invasion.....22

2.4.4 Increased cellular contractility extends survival time in an orthotopic mouse model.....30

2.5 Discussion.....32

2.6 Acknowledgements.....34

**Chapter 3: Concluding Remarks**.....35

3.1 Summary and significance.....36

3.2 Future work and final thoughts.....37

**References**.....40

# Acknowledgements

I am grateful to my family, friends, and mentors who helped me complete this journey.

Professionally, I thank my dissertation adviser Professor Sanjay Kumar, for his encouragement, guidance, and scientific expertise. I thank Professor Tejal Desai and Professor Daniela Kaufer for serving on my dissertation committee, and for their support and guidance with this work. I thank Dr. Loic Deleyrolle and Dr. Brent Reynolds from the University of Florida for their scientific expertise and contributions to this work. I thank Professor Song Li, Professor David Schaffer, Professor Amy Herr, and Professor Steve Conolly for their encouragement and helpful career advice. I thank past and present colleagues from the Kumar Laboratory for providing thoughtful feedback on my research and being helpful lab mates. I also thank my undergraduate research mentors Professor Markus Buehler, Professor Subra Suresh, and Dr. David Quinn for introducing me to academic research and inspiring me to pursue a Ph.D. I thank my undergraduate and graduate industry internship supervisors Dr. Ayyana Chakravartula and Dr. Kui Liu, respectively, for being wonderful mentors and for sharing their philosophies on life. Lastly, I thank the following funding agencies for providing financial support: California Institute for Regenerative Medicine (CIRM), Cancer Research Coordinating Committee (CRCC), and Siebel Scholar Foundation.

Personally, I thank all of my friends within the graduate program and outside of graduate school who have made earning a Ph.D. worth the journey. I will try my best to keep this list brief, and I apologize if I missed anyone. I thank Theresa Ulrich and Albert Keung for their friendship, support, and being wonderful role models. I thank fellow BEAST Presidents Anchi Tsou, Anuj Patel, Laura Rose Croft, John Waldeisen, Joseph Wilson, Lukasz Bugaj, Christine Leon-Swisher, and Paul Keselman for their camaraderie and for leading the best student group ever. I thank Elisabet Rosàs, Hector Neira, John Kim, Kevin Yamauchi, Julea Vlassakis, Jung-Ming George Lin, Ginny Kang, and Robert Lin for making every day enjoyable and for the unforgettable food outings. I thank Jorge Santiago-Ortiz for being a wonderful collaborator and for being the bright sunshine that keeps me smiling throughout the day. I thank Sean McFarland, Wiktor Stopka, Arunan Skandarajah, Dawn Spelke, Kate Miroshnikova, and Win Pin Ng for the amazing brunches, hikes, and camping adventures. I thank Genia Vogman for her companionship on the tennis courts. I thank Laura Walsh and Alex Tanielian for organizing the weekly game nights. I thank Timothy Downing, Jeff Henry, Yue Geng, and Tait Takatani for their invaluable career advice. I thank Kimberly Kam and Meiling Gao for being wonderful friends and for their unwavering support. I especially thank Monica Kapil for being such a compassionate friend, and always supporting and looking out for me.

Finally, I thank my mother Mei, my father Chiming, my brother Yilok, my mother-in-law Dorian, my father-in-law Doug, my sister-in-law Diana, and my relatives in the U.S. and in Hong Kong for their continued support of my ambitions. The most significant acknowledgement goes to my husband, Donald. I cannot imagine my life without him and know for a fact that this body of work would have never been completed without his love and support.

# Chapter 1: Introduction to matrix regulation of tumor-initiating cells

Reprinted with permission from Elsevier, from Chapter 10 in *Progress in Molecular Biology and Translational Science* 126: 243-256, "Matrix regulation of tumor-initiating cells", by Sophie Y. Wong and Sanjay Kumar.

©2014 Elsevier

doi: 10.1016/B978-0-12-394624-9.00010-5

## 1.1 Abstract

The recognition that the progression of many tumors may be driven by specific subpopulations of cells with stem/progenitor-like properties (tumor-initiating cells or TICs, a.k.a. cancer stem cells) represents an important recent paradigm shift in cancer biology and therapeutics. TICs in solid tissues are expected to interface with the extracellular matrix (ECM), which can strongly influence cell behavior through a variety of biochemical and biophysical mechanisms. Understanding ECM regulation of TIC behavior is important for developing strategies to isolate, expand, and characterize TICs in a laboratory setting and for understanding the roles ECM-based inputs may play in disease progression and therapy. In this chapter, we discuss how the ECM regulates TICs, starting with a brief overview of TIC biology, isolation, and characterization, molecular mechanisms through which TICs may be regulated by ECM-based signals, and the potential importance of these signals to TIC-driven tumor progression and metastasis.

## 1.2 Introduction

It is an unfortunate reality in cancer that a single treatment strategy is rarely if ever effective for all patients at all times. For example, a chemotherapeutic regimen that initially produces tumor regression may fail later as a resistant population of tumor cells emerges. Moreover, two patients with clinically and histologically similar tumors may exhibit dramatically different responses to a given chemotherapeutic regimen depending on the genomic and proteomic profile of the patient and tumor. This immense heterogeneity between and within tumors frustrates efforts to identify reliable molecular and cellular targets and thus represents a key therapeutic barrier to treatment (1–3). While the nature and implications of this heterogeneity remain incompletely understood, one important and recently appreciated manifestation of this heterogeneity is the variable ability of cells within a given tumor to propagate the tumor and seed new tumors. In particular, it is becoming clear that for many tumors, a privileged and comparatively rare subpopulation of cells is uniquely able to seed new tumors, whereas the vast majority of tumor cells, presumably this rare subpopulation's more differentiated progeny, contribute to the tumor "bulk" (Figure 1.1). In this sense, this tumor-initiating subpopulation shares conceptual similarities with stem or progenitor cells, in that these cells can both self-renew and differentiate to yield more specialized progeny.

Some of the first evidence that a population of cancer cells may have stem-like capabilities emerged in 1994 when Lapidot and colleagues found that only the $CD34^{+}/CD38^{-}$ subpopulation of leukemia cells generated new tumors in mice (4). The authors also found that the frequency of immature tumor cells was 1000 times less than mature tumor cells, suggesting that this tumor-initiating population could be rare. These findings led to what the field now recognizes as the cancer stem cell (CSC) hypothesis (5–7), which states that a subpopulation of tumor-initiating cells (TICs) is more tumorigenic than the rest of the tumor cell population and is capable of recapitulating all components of the tumor (e.g. those involved in growth, invasion, and metastasis) and may be highly resistant to therapeutics. TICs have been identified in several cancers including breast cancer (8,9), prostate cancer (10,11), lung cancer (12), and brain cancer (13,14). These cells now go by many names, including TICs, CSCs (6,15,16), and tumor-propagating cells. Whatever the terminology, the common concept is that these cells share key

functional properties of stem cells and can initiate new tumors when introduced in small numbers to tumor-free tissue. Most importantly, TICs can initiate and propagate tumors that are histologically equivalent to their tumors of origin when orthotopically implanted into immunocompromised animals.

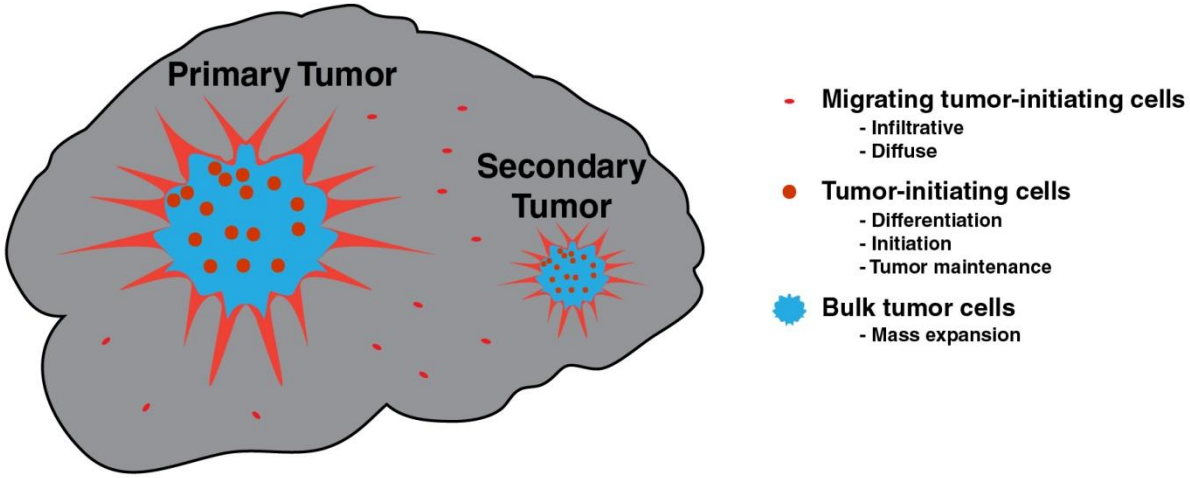


**Figure 1.1: Tumor-initiating cells drive secondary tumor formation.** Tumors are recognized to consist of a highly heterogeneous population of cells, only some of which can propagate and seed new tumors. This population of tumor-initiating cells (TICs) can diffusely infiltrate tissue (in this example, brain parenchyma), leading to secondary tumor formation. TICs also give rise to more differentiated progeny, which can both add to the tumor "bulk" as well as contribute to more specialized stromal functions such as angiogenesis.

### 1.3 Significance of TICs

In addition to lending fundamental new insight into the pathophysiology of tumor progression, a deeper understanding of TIC biology may accelerate the optimization and discovery of treatment regimens. There are at least two ways in which deeper engagement of TICs could aid therapy: first, the development of modalities that directly and specifically target TICs would theoretically represent the most effective way to contain or eradicate a tumor. For example, even after surgical resection of a primary tumor and aggressive follow-up chemo- and/or radiation therapy, the tumor would be expected to recur if a small number of TICs are left behind that could seed new tumors, perpetuate angiogenesis, and invade surrounding tissue. In principle, precise neutralization of TICs would effectively stop tumor initiation (17). Second, TICs offer a route to personalized medicine, in that they may be specifically isolated from a given patient's tumor and used for patient-specific molecular profiling, drug screening, and disease modeling. Molecular sequencing technologies can be combined with tumor sampling techniques to quantify tumor heterogeneity, trace cell population ancestry, and measure tumor-specific characteristics. For example, Sottoriva and colleagues (18) developed a framework that could generate patient-specific profiles days after tissue collection and did not require xenotransplantation. TIC characteristics considered in this model included a variety of factors such as: fraction of TICs in

the tumor, TIC symmetric division rate, methylation/demethylation rate per cell division, relative tumor age from malignant transformation, and rate of apoptosis. The modeling results matched those reported from xenotransplantation assays, supporting the clinical relevance of this model and its potential for designing patient-specific treatments.

The role of TICs in driving glioblastoma (GBM) has been an especially active area of study. GBM is the most aggressive primary brain tumor and has a median survival time of about 15 months, even with surgery and aggressive chemo- and radiotherapy (19). A variety of laboratories have isolated subpopulations of TICs from GBM tumors that can recapitulate characteristics of the original tumor when transplanted into immunocompromised mice, such as migratory and infiltrative capabilities, nest-like formations, vascular proliferation, nuclear pleomorphism with mitotic figures, and areas of pseudo-palisading necrosis (5,6,20–24). The continuous cell lines that have been extensively used as culture models of GBM (e.g. U87-MG) typically grow in vivo by direct expansion and do not recapitulate the infiltrative character and other key histologic features of the original tumor when transplanted into mice (22–25). Thus, while these lines may adequately capture more differentiated elements of the tumor that primarily participate in tissue infiltration, TICs may serve as a more clinically relevant model for investigating cellular aspects of the initiation and maintenance of GBM.

A number of studies have supported a role for TICs in tumor propagation (26) and correlated TIC presence with clinical outcome (27,28). One study used matched TIC and non-stem tumor cells and followed the single cells from injection to tumor growth to show that TICs are more tumorigenic than more differentiated tumor cells (26). The TICs proliferated faster than the nonstem tumor cells and more fully recapitulated tumor heterogeneity. Furthermore, analysis of secondary tumors contained a high population of TICs and their progeny. A clinical study that compared expression of the TIC marker CD133 (see below) and patient outcome using a panel of 95 gliomas found that high-grade glioma is strongly associated with high CD133 expression. This study also found that high frequency and clusters of CD133 positive cells—independent of tumor grade, extent of resection, and patient age—could be prognostic factors for gliomas (27). Finally, another study found that low-grade gliomas have low expression of the neural stem cell marker nestin, whereas more aggressive, high-grade gliomas have higher nestin expression and produce shorter survival times. Xenotransplantation of tumor-derived spheroids in mice gave rise to tumors in which nestinpositive cells localized to the invasive front (28).

### 1.4 Identification and isolation of TICs

Manipulation of TICs in culture presupposes an ability to reliably identify and isolate these cells. As a result, much effort has been devoted to the search for sensitive and specific TIC markers that may be exploited in flow cytometry, fluorescence-activated cell sorting, immunofluorescence, and other applications. For identification and isolation of GBMTICs, many studies have used neural stem cell surface markers such as CD133 (29), CD15 (30), and A2B5 (31). Similarly, the integrin subunit α6 was shown to be expressed at high levels in GBM TICs and to play a functional role in GBM TIC maintenance and tumor formation capacity (32). Although several markers have been identified, use of any one marker alone has proven to be somewhat unreliable. For example, both$CD133^{+}$ and$CD133^{-}$ glioma cells can display stem-like

properties and can generate secondary tumors in orthotopic mouse models (33,34). As a result, while the field continues to search for sensitive and specific molecular markers, the gold standard for verification of GBMTICs remains a functional one—i.e., GBMTICs are defined by their ability to recapitulate the tumor of origin when orthotopically implanted into immunocompromised mice. A variety of in vitro functional screens have been developed to streamline and augment in vivo implantation studies. For example, cell survival in neural stem cell medium over several passages has been successfully used to select GBM TICs from bulk tumor tissue (20). Another study exploited the inverse correlation between proliferation rate (cell cycling speed) and tumorigenicity to select for GBMTICs (5,35). Improved characterization of TIC properties and the development of new screening/isolation methodologies are critical for further studies that seek to better understand tumor pathogenesis.

### 1.5 Role of extracellular matrix and mechanical signals in regulating TIC function

Having described the identification and isolation of GBM TICs, we now turn to a more detailed discussion of how the extracellular matrix (ECM) may regulate TIC behavior, with a special focus on GBM. In GBM, it is now evident that TICs invade along perivascular spaces, which have a high concentration of ECM proteins such as collagen, fibronectin, and laminin (36). TICs sense and process these matrix-bound factors through adhesion receptors such as integrins (32,37) and CD44 (38). For example, Lathia and colleagues discovered that integrin α6, a laminin receptor, is necessary for TIC survival and proliferation and directly correlates with TIC stem cell marker expression (32). Another recent study showed that integrin α3, which adheres to laminin and fibronectin, is overexpressed in CD133-positive TICs. Suppression of α3 slowed random migration and reduced transwell invasion in glioma cell lines, which in turn depended on ERK1/2 phosphorylation (37). In addition to integrins, the adhesion receptor CD44 has been widely studied and characterized in multiple cancers (39). High expression of CD44 in GBM TICs correlates with poor clinical prognosis and has been shown to regulate TIC growth through Akt and other signals (38,40). These adhesion receptor studies support an important role of ECM in TIC function and tumorigenesis.

While these and other studies clearly demonstrate that ECM ligation can trigger signals that modulate TIC behavior, it has also become clear over the past two decades that mechanical cues encoded within the ECM can also direct tumor invasion and growth. Features within the ECM such as matrix geometry, density, and rigidity have been shown to regulate fundamental cellular functions such as motility, proliferation, and gene expression (41–45). For example, endothelial cells and fibroblasts have higher cell spreading area and motility on stiff matrices when compared to soft matrices (44,46). It has also been shown that continuous GBM culture models have increased motility, spreading area, and proliferation on stiff matrices (41). Interestingly, differences in ECM rigidity can also direct the differentiation of adult stem cells, including mesenchymal and neural stem cells (42,47). In the first and perhaps bestknown such study, Engler and colleagues showed that mesenchymal stem cells preferentially undergo neurogenesis on soft ECMs ranging in stiffness from 0.1 to 1 kPa, myogenesis on ECMs ranging from 8 to 17 kPa, and osteogenesis on stiff ECMs ranging from 25 to 40 kPa (42). They also found that inhibition of nonmuscle myosin II blocked differentiation, thus implicating myosin-based contractile signaling in stiffness-dependent differentiation. Later, Keung and colleagues showed

that soft matrices (0.1–0.7 kPa) directed neural differentiation of adult neural stem cells, whereas stiff matrices (1.5–75 kPa) produced relative enrichment of astrocytic differentiation (48). Mechanistic studies then revealed that the GTPases RhoA and Cdc42 were key to these effects, with suppression of these proteins rescuing neuronal differentiation on stiff ECMs.

### 1.6 Propagation of TICs in ECM-adherent cultures

Since the ECM can instruct or select for specific cellular behaviors, it is important to consider the role the ECM may play in culturing TICs in the laboratory setting (49). For example, GBM TICs can be grown in adherent cultures (21) or as neurospheres in suspension (50,51) (Figure 1.2). While TICs were long thought to retain their tumor-initiating capacity only when propagated long term as neurospheres, more recent studies reveal that TICs may be propagated as adherent cultures without loss of marker expression or tumor-initiating capacity (21,22). Specifically, the authors of this study verified the tumorigenicity of each adherent TIC line by injecting 100,000 TICs intracranially into immunocompromised mice. After the mice were sacrificed, the resulting tumors had infiltrated brain tissue and expressed characteristic molecular markers (e.g. nestin) and displayed histopathological hallmarks of GBM. Remarkably, limiting dilution studies revealed that some TIC lines could form aggressive tumors upon transplantation of as few as 100 cells. In addition, adherent cells could be differentiated in culture into marker-positive neuronal, oligodendrocytic, and astrocytic lineages. Some important practical advantages of adherent culture over neurosphere culture include more straightforward quantification of cell proliferation, improved cellular homogeneity, and fewer gradients in oxygen, nutrients, and other soluble factors. Perhaps most importantly, the adherent culture paradigm facilitates high-throughput screening; to illustrate this, the authors screened their TIC lines with 450 drugs from the NIH Clinical Collection and found that 23 of these drugs killed all TIC lines tested, including, unexpectedly, seven agents that target monoamine signaling (e.g. serotonin-specific reuptake
inhibitors).

This is not to say that TICs in a small neurosphere (e.g. 150–200 μm) cannot maintain stem-like properties; however as the neurosphere grows larger, the percentage of stem-like cells rapidly decreases (49), which has been ascribed to the increasingly uneven access to growth factors and oxygen as the neurosphere grows and may be further complicated by increases in juxtacrine and paracrine signaling. In adherent culture, all cells have effectively equal access to soluble factors in the medium, and cells may be plated at sufficiently low density as to minimize cell–cell contacts. In addition, the increased exposure to laminin in the matrix can promote maintenance of stem-like properties for adherent cells, which has been found to be an important factor in identifying TICs (32). Although debate continues about which culture method is best for a given application, both are used to successfully propagate TICs *in vitro*.

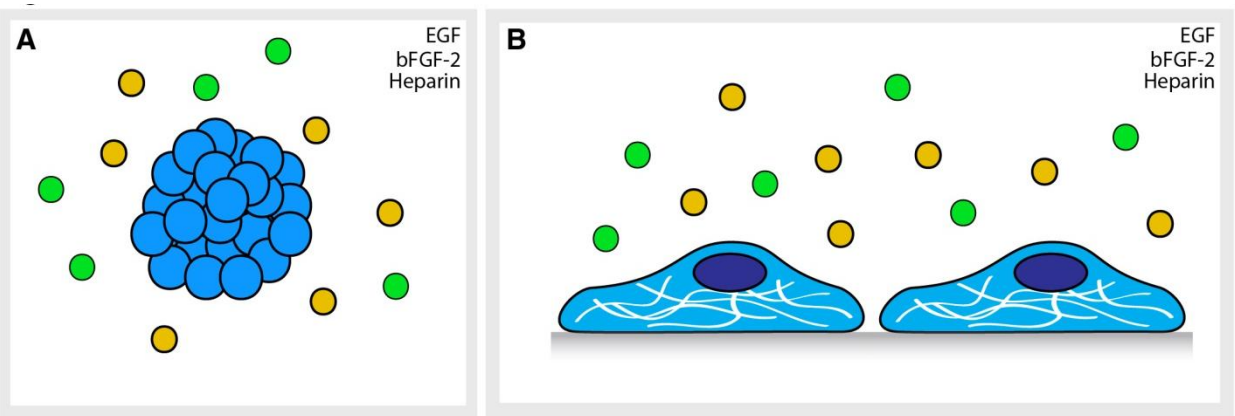


**Figure 1.2: Comparison of adherent and neurosphere-based TIC cultures.** Both neurosphere and ECM-adherent cultures are widely used to propagate TICs. (A) An acknowledged limitation of neurosphere culture is the possibility of gradients across the sphere in oxygen, nutrients in the culture, and cell-secreted factors, as well as uneven access to extracellular matrix. (B) Adherent culture has recently emerged as a complementary paradigm to neurosphere culture, with the prospect of minimizing these gradients while also offering greater scalability.

## 1.7 Mechanisms of mechanotransduction

The finding that TIC behavior is regulated by ECM engagement and biophysical properties raises the question of whether the molecules that mediate these effects may bear value as drug targets. For example, Cilengitide, an $\alpha_v$ integrin antagonist, inhibits GBM growth in preclinical models and is currently being evaluated in clinical trials (52). Recent studies with breast and prostate cancer have used integrins to select for a tumor-initiating subpopulation from the bulk tumor (8,11). As described earlier, the laminin receptor integrin α6 is highly expressed in GBM TICs and is necessary for BTIC selfrenewal, proliferation, and tumor formation capacity (32). Since laminin is abundant in the BTIC perivascular niche, this result is significant because it suggests a mechanism through which this ECM protein can contribute to maintenance of stemness.

Several actin binding proteins (53,54) and transcription factors relevant to integrin signaling and mechanotransduction (55–58) have been identified to have the capability of regulating GBM initiation, invasion, and chemosensitivity. For example, the transcription factor ZEB1 is highly expressed in GBM TICs and is known to be correlated with shorter survival and poor response to Temozolomide (58,59). ZEB1 is regulated by tyrosine receptor type A, and increased expression leads to increased binding to E-box regions of E-cadherin, resulting in highly motile cells and increased tumor invasion. Downstream targets of ZEB1 have subsequently been shown to include ROBO1, OLIG2, CD133, and MGMT. Knockdown of ZEB1 sensitizes cells to temozolomide and decreases expression of stem cell markers SOX2, OLIG2, and CD133 (58).

Another example is the influence of the actin binding protein, Girdin, which is activated by the PI-3-Kinase/Akt pathway. Activation of the Akt pathway can induce conversion from low-grade to high-grade glioma and regulates angiogenesis, apoptosis, and invasion (60,61). Girdin is known to regulate cell migration, cell polarity, and epithelial–mesenchymal transition, and in

GBM TICs contributes to self-renewal and tumorigenicity (54). Tumor grade is positively correlated with Girdin expression, and knockdown of Girdin decreases motility and invasion, neurosphere formation, tumorigenicity, and expression of nestin and CD133, and induces differentiation. These studies collectively show that tumor initiation, invasion, and chemoresistance are linked by pathways that are activated by biochemical and potentially mechanical factors in the ECM.

Liu and colleagues recently tied together these concepts by showing that the composition and mechanics of the ECM used to culture TICs can exert powerful instructive and/or selective effects that can profoundly influence subsequent tumorigenicity (62). The authors examined the formation of melanoma TICs in 3D fibrin gels of varying stiffnesses and found that the softest gel (0.09 kPa) generated the most and largest spheroids over a 5-day period when compared to the stiff gel (1.05 kPa). Subcutaneous transplantation of TICs propagated in the soft gel resulted in greater primary tumor formation and lung metastasis compared to TICs propagated on hard plastic. Furthermore, spheroids grown in the soft gel exhibited increased expression of stem cell markers CD133, nestin, and Bmi-1.

## 1.8 Discussion

While it has long been recognized that tumors are highly heterogeneous, only recently has it been appreciated that this heterogeneity may reflect a hierarchy of cellular entities in which a comparatively rare subpopulation of TICs are capable of initiating and propagating the tumor. Over the past decade, significant effort has been devoted to identifying and clarifying the function of these TICs, which has allowed investigators to dissect specific contributions of individual factors to tumor progression. As described in this review, the field is only beginning to understand the importance of the ECM and other solid-state components of the microenvironment in regulating TIC behavior, and there is every reason to expect that mechanical inputs will prove to be an important dimension of this regulation. As our understanding of the role of ECM and mechanical signals to TIC biology advances, there are several open questions to address, each of which presents important opportunities to innovate. First, what are the defining characteristics of the TIC physical microenvironment *in vivo*, how is this different from the normal tissue microenvironment, and which characteristics are most important to tumor initiation and propagation? Second, if mechanical inputs are important to TIC function, how do the signaling systems that process these inputs interface with more canonical oncogenic signaling systems? Specifically, can aberrant mechanotransductive signaling "tip the balance" between TIC quiescence and tumorigenesis, and could this be leveraged in some way to identify new druggable targets? Third, combining these concepts, is it possible to develop advanced *in vitro* culture systems that enable one to investigate ECM and mechanobiological regulation of TICs in a systematic, high-throughput, and physiologically mimetic fashion? One envisions that advances in this last area could dramatically accelerate both fundamental discovery and therapeutic design, with standardized culture platforms serving as key enabling technologies for personalized molecular and chemotherapeutic screening. Realizing this vision will require a highly multidisciplinary effort, including input from biomaterials scientists, micro- and nanotechnologists, cell and ECM biologists, and of course cancer biologists. The coming years and decades are likely to be extremely exciting ones for this field, with advances in basic

science directly informing technology and therapeutics and therapeutic advances opening new avenues for scientific inquiry.

# Chapter 2: Constitutive activation of Myosin-dependent contractility sensitizes glioma tumor-initiating cells to mechanical inputs and reduces tissue invasion

Reprinted with permission from the American Association for Cancer Research, from the article, "Constitutive activation of Myosin-dependent contractility sensitizes glioma tumor-initiating cells to mechanical inputs and reduces tissue invasion", by Sophie Y. Wong, Theresa A. Ulrich, Loic P. Deleyrolle, Joanna L. MacKay, Jung-Ming G. Lin, Regina T. Martuscello, Musa A. Jundi, Brent A. Reynolds, and Sanjay Kumar in *Cancer Research*, 75(6): 1113-22, 2015.

©2015 by the American Association for Cancer Research

doi: 10.1158/0008-5472.CAN-13-3426

## 2.1 Abstract

Tumor-initiating cells (TIC) perpetuate tumor growth, enable therapeutic resistance, and drive initiation of successive tumors. Virtually nothing is known about the role of mechanotransductive signaling in controlling TIC tumorigenesis, despite the recognized importance of altered mechanics in tissue dysplasia and the common observation that extracellular matrix (ECM) stiffness strongly regulates cell behavior. To address this open question, we cultured primary human glioblastoma (GBM) TICs on laminin-functionalized ECMs spanning a range of stiffnesses. Surprisingly, we found that these cells were largely insensitive to ECM stiffness cues, evading the inhibition of spreading, migration, and proliferation typically imposed by compliant ECMs. We hypothesized that this insensitivity may result from insufficient generation of myosin-dependent contractile force. Indeed, we found that both pharmacologic and genetic activation of cell contractility through RhoA GTPase, Rho-associated kinase, or myosin light chain kinase restored stiffness-dependent spreading and motility, with TICs adopting the expected rounded and nonmotile phenotype on soft ECMs. Moreover, constitutive activation of RhoA restricted three-dimensional invasion in both spheroid implantation and Transwell paradigms. Orthotopic xenotransplantation studies revealed that control TICs formed tumors with classical GBM histopathology including diffuse infiltration and secondary foci, whereas TICs expressing a constitutively active mutant of RhoA produced circumscribed masses and yielded a 30% enhancement in mean survival time. This is the first direct evidence that manipulation of mechanotransductive signaling can alter the tumor-initiating capacity of GBM TICs, supporting further exploration of these signals as potential therapeutic targets and predictors of tumor-initiating capacity within heterogeneous tumor cell populations.

## 2.2 Introduction

Glioblastoma (GBM) is the most aggressive primary brain tumor and is characterized by poor survival even in the setting of surgery, radiation, and chemotherapy (19). Diffuse invasion of single cells within the parenchyma and along vascular structures frequently renders complete surgical resection impossible and leads to recurrence and eventual mortality. This in turn has motivated much effort to understand mechanisms of GBM invasion, an important goal of which is to discover potential molecular targets that could be manipulated to slow disease progression (63,64). Although soluble and cell-bound factors have long been recognized as important regulators of tumor invasion, it has only recently become clear that biochemical and biophysical cues encoded in the extracellular matrix (ECM) can also strongly regulate tumor invasion. For example, in previous work, we showed that ECM rigidity can regulate GBM cell adhesion, motility, and proliferation, which in turn requires the contractile activity of myosin II (41), as well as the cell–ECM adhesion proteins α-actinin (65) and talin-1 (66). More specifically, when GBM tumor cells are cultured on comparatively stiff ECMs, they spread and migrate very readily whereas they adopt a rounded and immotile phenotype on highly compliant (soft) ECMs. This is consistent with observations in other tumor types that ECM stiffening can promote tissue dysplasia and local invasion through integrin-dependent potentiation of cell–ECM adhesion (67–69).

Much of our understanding of the importance of cell–ECM mechanotransduction in tumor progression is based on the use of continuous cell lines or, less commonly, heterogeneous primary tumor samples that are derived from the bulk tumor. Although these studies have provided much valuable mechanistic insight, it has become clear over the past decade that a very specific and comparatively rare subpopulation of cells plays especially key roles in populating the tumor and driving tumor recurrence following chemo- and radiotherapy. In the case of GBM, these tumor-initiating cells (TIC) are formally defined by their ability to recapitulate the original tumor when orthotopically xenografted into immunocompromised mice and are characterized by expression of a specific complement of molecular markers (e.g., CD133, nestin) and stem cell-like properties of self-renewal and differentiation into various tissue lineages. In addition to repopulating tumors, TICs directly participate in the invasion process *in vivo*. For example, both primary GBM TICs (5) and H-Ras-transduced neural stem cells (70) invade brain tissue before forming the tumor mass. Moreover, hypoxia, which is often associated with the TIC niche (71) and the necrotic tumor core in which GBM TICs may reside, can enhance migration of GBM tumor cells through induction of the family of hypoxia-inducible factors (72,73).

Invasive motility through tissue is a physically integrated process that requires tumor cells to sense ECM-based mechanical inputs, dramatically change their shape, and exert propulsive forces against the microenvironment (63,74). Interestingly, many TIC markers such as Oct 3/4 (55) and SOX2 (56,57) have been shown to regulate cell behaviors that require cell–ECM mechanotransduction, such as motility and invasion. Conversely, several proteins long known for their adhesive or cytoskeletal function have more recently been discovered to be highly enriched and functionally important in TICs, such as the actin-binding protein girdin (54), the α6 integrin subunit (32,75), and the hyaluronan receptor CD44 (76) and its effector moesin (38).

These and other studies led us to speculate that cell–ECM mechanotransductive signaling systems play key roles in the ability of GBM TICs to interact with brain ECM and infiltrate tissue, and that targeting these systems may limit tumor growth and progression *in vivo*. Here, we explore this important open question by combining materials fabrication, single-cell biophysical tools, *in vitro* characterization of primary GBM TICs, and mouse xenograft models. We show that GBM TICs are capable of evading restrictions on spreading, motility, and self-renewal normally imposed by ECMs with compliance comparable with brain tissue, and that this mechanosensitivity may be restored by activation of myosin-dependent contractility. This contractile activation has the additional effect of limiting tumor invasion in a mouse orthotopic xenograft model and dramatically enhancing survival. Our work establishes the importance of cell–ECM mechanotransductive signaling in the initiation of GBM tumors and suggests a new set of molecular targets that may be manipulated to limit tumor infiltration.

## 2.3 Materials and Methods

### 2.3.1 Tumor sample and primary cell culture

The two patient-specific human brain tumor samples used in this study, L0 and L2, were collected in a previous study (5) after informed consent from male patients who underwent surgical treatment and Institutional Review Board approval. Briefly, the extracted tissue was

placed in an enzymatic cocktail containing trypsin/ethylenediaminetetraacetic acid (0.05%) for 10 minutes at 37°C and filtered through a 40 μm filter. Cells were then propagated in neurosphere assay growth conditions (50) with serum-free media (Neurocult NS-A Proliferation kit, Stem Cell Technologies) that contained EGF (20 ng/mL, R&D), basic fibroblast growth factor (bFGF, 10 ng/mL, R&D), and heparin (0.2% diluted in PBS, Sigma). The tumor cells form gliomaspheres in suspension under these culture conditions and were serially passaged every 5 to 7 days when spheres reached a diameter of about 150 μm according to a previously established protocol (5). Gliomaspheres were dissociated with trypsin/ethylenediaminetetraacetic acid (0.05%) for 2 minutes and then replated in fresh media with addition of EGF, bFGF, and heparin. Both lines used were only passaged less than 20 times. These cells have been transcriptionally characterized and classified as the Classical subtype of GBM (58). Short tandem repeat (STR) analysis (University of Arizona Genetics Core; Tucson, AZ) confirmed that these cells had not been contaminated by any known cell lines.

### 2.3.2 Continuous cell line culture

U373-MG human GBM cells were obtained from the University of California, Berkeley (Berkeley, CA) Tissue Culture Facility in 2007, which obtained its cultures directly from the ATCC in 1995. Frozen stocks were made immediately upon receipt, and cultured for less than 6 months for experiments. We note that STR analysis has recently revealed that ATCC U373-MG cells share a common origin with the U251-MG glioma cell line (77), although these lines may have subsequently diverged to exhibit differential drug sensitivities (78). The tumor cells were cultured adherently in DMEM (Life Technologies) supplemented with 10% calf serum (J.R. Scientific), 1% penicillin/streptomycin, MEM nonessential amino acids, and sodium pyruvate (Life Technologies).

### 2.3.3 Identification of slow-cycling population using CFSE and flow cytometry

As reported previously (5), carboxyfluorescein diacetate succinimidyl ester (CFSE) can be loaded into brain tumor-initiating cells to identify slow-cycling subpopulations. A Cell Trace CFSE Cell Proliferation Kit (Invitrogen) was used to load the dye into the tumor cells. TICs were trypsinized before fluorescence was measured using an FC-500 flow cytometer (Beckman Coulter), and results were analyzed by using FlowJo. The top 5% of CFSE bright cells were defined as the slow-cycling subpopulation.

### 2.3.4 Differentiation of brain tumor-initiating cells

A previously established protocol for differentiating TICs was followed (5). Briefly, 5% calf serum was added to basal culture media that lacked growth factors. After 7 to 10 days, expression of lineage markers was assayed using immunofluorescence. For BMP-4–induced differentiation (Figure 2.S2), TICs were incubated with BMP-4 (100 ng/mL; R&D Systems) in the absence of growth factors (bFGF, EGF, heparin) in adherent culture for 48 hours (79).

### 2.3.5 Synthesis and functionalization of extracellular matrices

Polyacrylamide 2D matrices were synthesized following our previously described protocol (41) and functionalized with natural mouse laminin (10 mg/ml, Invitrogen). Matrices with elastic moduli of 0.08, 0.80, and 119 kPa contained final acrylamide/*bis*-acrylamide (A/B) percentages of 3% A/0.05% B, 5% A/0.1% B, and 15% A/1.2% B, respectively, as measured in Urlich et al. (2009). All analyses were conducted on data pooled from at least three technical and three biological (gel) replicates.

### 2.3.6 Phase and epifluorescence imaging and immunofluorescence staining

All live-cell and fluorescence imaging was performed using either an inverted Nikon TE2000-E2 or a Nikon Ti-E microscope equipped with a motorized, programmable stage (Prior Scientific, Inc. and Applied Scientific Instrumentation), an incubator chamber to maintain constant temperature, humidity, and $CO_2$ levels (*In vivo* Scientific), a digital camera (Photometrics Coolsnap HG II, Roper Scientific), and SimplePCI (Hamamatsu Corporation) and NIS Elements (Nikon Instruments, Inc.) software. Cells were fixed and stained for filamentous actin (F-actin), vinculin, and the nucleus as previously described (41). Cell spreading measurements were obtained by quantifying the area of cells using Image J software (NIH). Epifluorescence images obtained in Figs. 1, 2, 3, 7, and S1 were enhanced by adjustments to brightness and contrast as necessary to reduce background signal. The following primary antibodies were used for immunofluorescence: anti- vinculin (1:500, Sigma-Aldrich), anti-glial fibrillary acidic protein (1:500, Dako), anti-human Nestin (1:500, Millipore), TUJ1 (1:1000, Promega), and anti-human SOX2 (1:500, R&D). F-actin and nuclei were stained with phalloidin (1:200, Invitrogen) and 4',6-diamidino-2-phenylindole (1:200, Invitrogen), respectively.

### 2.3.7 Measurement and analysis of cell motility

Following a previously established protocol, we measured cell motility using 10X phase contrast timelapse images acquired every 15 minutes over a 12h period (41). At least 10 representative fields of view per substrate and at least three substrates per stiffness condition were used for analysis. ImageJ software (NIH) was used to track the centroid of each cell throughout the time sequence.

### 2.3.8 Measurement of cell proliferation

Cell proliferation was measured using a BrdU Flow Kit (BD Biosciences) according to the manufacturer's directions and analyzed with an FC-500 flow cytometer and FlowJo software. At least 3 technical and 3 biological replicates were analyzed per stiffness condition for each cell line. *In vivo* proliferation was measured using Ki67 antibody (1:500, Leica Biosystems) staining of tissue sections.

### 2.3.9 Constitutively active cell lines

Myc-tagged RhoA Q63L (80), Flag-tagged MLCK ED785-786KK (81) , and Myc-tagged ROCK1 D3(82) were subcloned into the lentiviral vector pSLIK containing the TRE tight doxycycline-inducible promoter, the reverse tetracycline transactivator (rtTA), and the YFP variant Venus (83). Viral particles were packaged in 293T cells and used to infect L0 and L2 brain tumor-initiating cells at a multiplicity of infection of 1 IU/cell. Cells expressing the pSLIK vector were sorted on a DAKO-Cytomation MoFlo High Speed Sorter based on Venus fluorescence. Control cell lines were created with the same method using empty vectors. Doxycyline was added at a concentration of 100 ng/ml 2-3 days prior to all experiments to activate the constitutively active constructs.

### 2.3.10 Western blot analysis

Western blots were performed as previously described (84), with minor modifications. Cells were lysed in RIPA buffer with protease inhibitor, phosphatase inhibitor, sodium fluoride, and sodium molybdate. Protein content was measured by BCA assay (Thermo Fisher Scientific) and normalized across samples. Lysates were boiled for 5 minutes, run on a 4-12% Bis-Tris gel, and transferred onto a PVDF membrane (Invitrogen). Primary antibodies used include anti-phospho-myosin light chain 2 (Thr18/Ser19) (1:1,000, Cell Signaling), anti-myosin light chain (1:5,000, Sigma-Aldrich), myosin II heavy chain isoform IIA (1:500,000, Covance), myosin II heavy chain isoform IIB (1:10,000, Covance), myosin II heavy chain isoform IIC (1:10,000, Covance), and anti-glyceraldehyde-3-phosphate dehydrogenase (anti-GAPDH) (1:1,000,000, Sigma Aldrich). Horseradish peroxidase-conjugated secondary antibodies (Invitrogen) and enhanced chemiluminescence reagent (Thermo Fischer Scientific) were used for protein detection on x-ray film or 555 fluorescent secondary antibody (1:1,000, Invitrogen) was used for protein detection using a Typhoon FLA 9500 biomolecular imager (GE Healthcare). Band intensities were quantified using the gel analysis plugin in ImageJ software (NIH) and normalized by GAPDH intensity.

### 2.3.11 Atomic force microscopy (AFM) protocol

AFM indentation measurements were performed as described earlier (84,85) using pyramid-tipped probes (OTR4, Bruker AFM Probes) and fitting force curves with a modified Hertz model. At least 30 cells cultured on glass were measured per condition.

### 2.3.12 Sphere forming frequency assay and sphere size measurement

Single cells were seeded onto non-adherent 384-well plates (Corning; 10 cells/well; 50µL media/well) using a Multidrop Combi microplate dispenser (Thermo Scientific). After 6-7 days, spheres were stained using Hoescht 33342 (1µg/ml, Sigma Aldrich) and imaged with the ImageXpress Micro cellular imaging system (Molecular Devices) in the CIRM/QB3 Shared Stem Cell Facility. Sphere forming frequency was obtained by dividing the number of observed

gliomaspheres in each well by the number of initially plated cells. Sphere sizes were measured using CellProfiler (Broad Institute).

### 2.3.13 Pharmacologic inhibition of cell motility

Non-muscle myosin-II inhibitor blebbistatin (25μM, Sigma-Aldrich) was added to the cell culture medium after cells were adhered for at least 3 hours.

### 2.3.14 Live/dead assay

Single cells were incubated with propidium iodide (0.5 mL/sample, BD Biosciences) for 15 min at room temperature as described in the manufacturer instructions. Flow cytometry analysis was conducted to determine percentage of live cells.

### 2.3.15 Mass spectroscopy quantification of NM II isoform expression

TICs cultured on gels were lysed as described above in Western blot analysis. Lysates with protein concentrations ranging from 0.548-1.306 mg/ml were submitted to the National Heart Lung and Blood Insitute Proteomics Core Facility (Dr. Robert Adelstein, NIH) for analysis by liquid chromatography tandem mass spectroscopy. Peptide numbers for each myosin-II heavy chain isoform were counted (86).

### 2.3.16 Collagen invasion assay

1.0 mg/ml collagen I gels (PureCol, Advanced Biomatrix) were assembled in a multiwell plate with 4-5 gliomaspheres implanted per gel. Phase images were taken every 24 hours with an inverted Nikon TE2000-E2 microscope.

### 2.3.17 Transwell migration assay

Transwell inserts with 3 μm pores (Fluoroblok, Fischer Scientific) were coated with laminin (10 mg/ml, Invitrogen), and a 2x gradient of soluble EGF was used to drive chemotaxis through the pores. Cells were allowed to migrate across the membrane for 24 hours before fixation with 4% paraformaldehyde (Electron Microscopy Sciences). Cell nuclei were fluorescently labeled with propidium iodide and cells adhered to the bottom surface of the membrane were counted using epifluorescence microscopy. At least 3 complete membranes were counted for analysis.

### 2.3.18 Xenotransplantation of human primary brain tumor-initiating cells into mice

Female 8-week-old nonobese diabetic/severe combined immunodeficient γ (NSG) mice (NOD.Cg-Prkdc(scid)Il2rg(tm1Wjl)/SzJ) were implanted intracranially with 200,000 L0 TICs (CA RhoA or Control) following institutional and national regulations, and according to a previously establish protocol (5). The mice were treated daily with doxycycline (625 mg/kg) beginning at 4 days after implant until endpoint. Five mice were used for each cohort and followed until death.

### 2.3.19 Immunohistochemistry

Mice brains were prepared for sectioning using paraffin, and haematoxylin and eosin staining was used to visualize tissue following standard protocols. Images were taken using an inverted Zeiss Axio microscope with a color camera (AxioCam ERc 5s, Zeiss).

### 2.3.20 Tumor occupancy measurement

Human GBM TICs were identified using an anti-human Nestin antibody (1:500, Millipore). Immunocomplexes were visualized in 3,3'-diaminobenzidine using the ABC-Elite peroxidase method (Vector Laboratories). Counterstaining of the nuclei was performed using hematoxylin. Tumor occupancy was estimated using the ImageJ (NIH) via calculation of the percent area occupied by the Nestin immunoreactive cells with the implanted brain.

### 2.3.21 Statistical analysis

Data are reported as mean ± SE. All pairwise statistical comparisons were performed with the Student unpaired *t* test, except as noted. Details of comparisons and replicates are provided in the appropriate figure legend.

## 2.4 Results

### 2.4.1 Tumor-initiating population is maintained on soft and stiff ECMs

Before asking whether ECM-encoded stiffness cues play instructive roles in regulating GBM TIC behavior, we first assessed the degree to which ECM stiffness might exert selective pressures that could compromise GBM TIC tumor-initiating or differentiation properties. To do this, we isolated two GBM TIC lines, L0 and L2, from human primary GBM tumors as previously described; unlike continuous culture models of GBM, these TICs generate tumors with pathologic hallmarks and invasion patterns of GBM when orthotopically xenografted in immunocompromised mice, even after multiple passages in culture (5). We then cultured these GBM TICs in neurobasal growth medium on laminin-coated polyacrylamide gels of rigidity varying from 0.08 kPa to 119 kPa (41). In a previous study, it was shown that the top 5% most slowly cycling GBM TIC fraction contained the most tumorigenic cells (5). To rule out the possibility that ECM rigidity might be selecting for or against this key subpopulation, we first

applied a serial dye dilution assay to measure the distribution of cell-cycling time (Figure 2.1A). Flow cytometry of carboxyfluorescein-treated cells revealed fluorescence distributions similar to previously reported results and highly overlapping across all ECM rigidities. This result indicates that a slow cycling, tumor-initiating subpopulation is preserved across all ECM rigidities (Figure 2.1A, arrow), prompting us to use the overall unsorted population for all subsequent studies. As additional evidence for an absence of selection, 100% of GBM TICs were found to express the self-renewal markers nestin and SOX2 (Figure 2.1B) and could be differentiated by serum into glial and neuronal marker-positive cells across all ECM rigidities (Figure 2.1C). Both cell lines demonstrated qualitatively similar behavior. Thus, alterations in ECM rigidity do not preferentially select for or against slow-cycling highly tumorigenic cells, alter stem cell marker expression, or compromise differentiation.

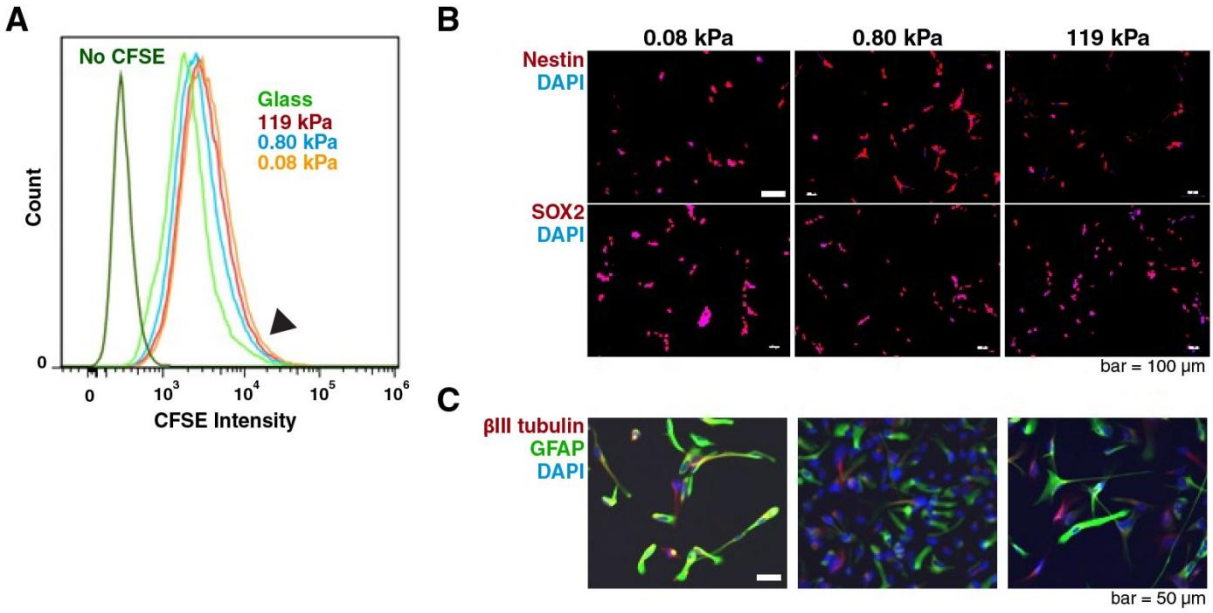


**Figure 2.1: Human primary GBM TICs retain stem-like properties when cultured on soft and stiff polyacrylamide gels coated with laminin.** (A) ECM stiffness does not select against slow-cycling GBM TICs. GBM TICs were treated with carboxyfluorescein diacetate succinimidyl ester (CFSE) and analyzed by flow cytometry to determine distribution of cycling rate. On the basis of the persistence of the high-CFSE shoulder (arrow), the slow cycling population is retained on all gel stiffnesses. L2 curves are shown; L0 displayed similar results. (B) GBM TICs also express the stem cell markers, nestin (top row; red; 100% positive) and SOX2 (bottom row; red; 100% positive) on all ECM stiffnesses. (C) all ECM stiffnesses permit neuronal and glial differentiation. Addition of 5% serum to GBM TIC cultures results in differentiation into glial (GFAP, green) and neuronal lineages (βIII tubulin, red).

### 2.4.2 Tumor-initiating cells can spread, migrate, and proliferate on soft and stiff ECMs

In previous studies with continuous human GBM cell lines, we demonstrated that soft ECMs comparable with brain tissue (0.08–0.8 kPa) can strongly limit cell spreading, motility, and proliferation (41). We therefore asked whether similar regulatory effects would be observed for GBM TICs. To our surprise, L2 TICs adopted the same elongated morphology on soft ECMs as on stiff ECMs (Figure 2.2A), with no significant differences in projected spread area (Figure 2.2B). Moreover, GBM TICs did not exhibit prominent stress fibers or mature focal adhesions (Figure 2.2C), structures strongly promoted by stiff ECMs in many other cell types (41,68,87). Qualitatively similar results were obtained for the L0 TIC line (data not shown). For both L0 and L2 TICs, random cell migration speed was only weakly sensitive to ECM rigidity (Figure 2.2D), whereas proliferation was completely insensitive to ECM rigidity, with GBM TICs robustly migrating and proliferating even on the most compliant matrices (Figure 2.2E). It occurred to us that the reduced stiffness sensitivity of GBM TICs relative to continuous GBM cell lines might simply be a consequence of the fact that GBM TICs are cultured in a neurobasal, serum-free medium, whereas continuous lines are typically cultured in a DMEM-based medium supplemented with 10% serum, which contains both ECM components and activators of adhesion and contractility (5,41). To rule out this possibility, we cultured the continuous human GBM cell line U373-MG in both neurobasal and DMEM-based medium with or without 10% serum supplementation and measured average cell speed across a range of ECM stiffnesses (Figure 2.S1). To assess correlations between stiffness-sensitivity and tumor-initiating capacity, we repeated the spreading and motility experiments with TICs after a brief (48 hours) treatment with bone morphogenetic protein 4 (BMP4), which has previously been shown to strongly inhibit tumorigenic potential (Figure 2.S1; ref. 79). Notably, BMP4 treatment restored ECM mechanosensitivity with respect to cell spread area but not motility, with the exception of L2 on the stiffest ECM. Additional characterization of the TICs were performed and can be found in the Appendix.

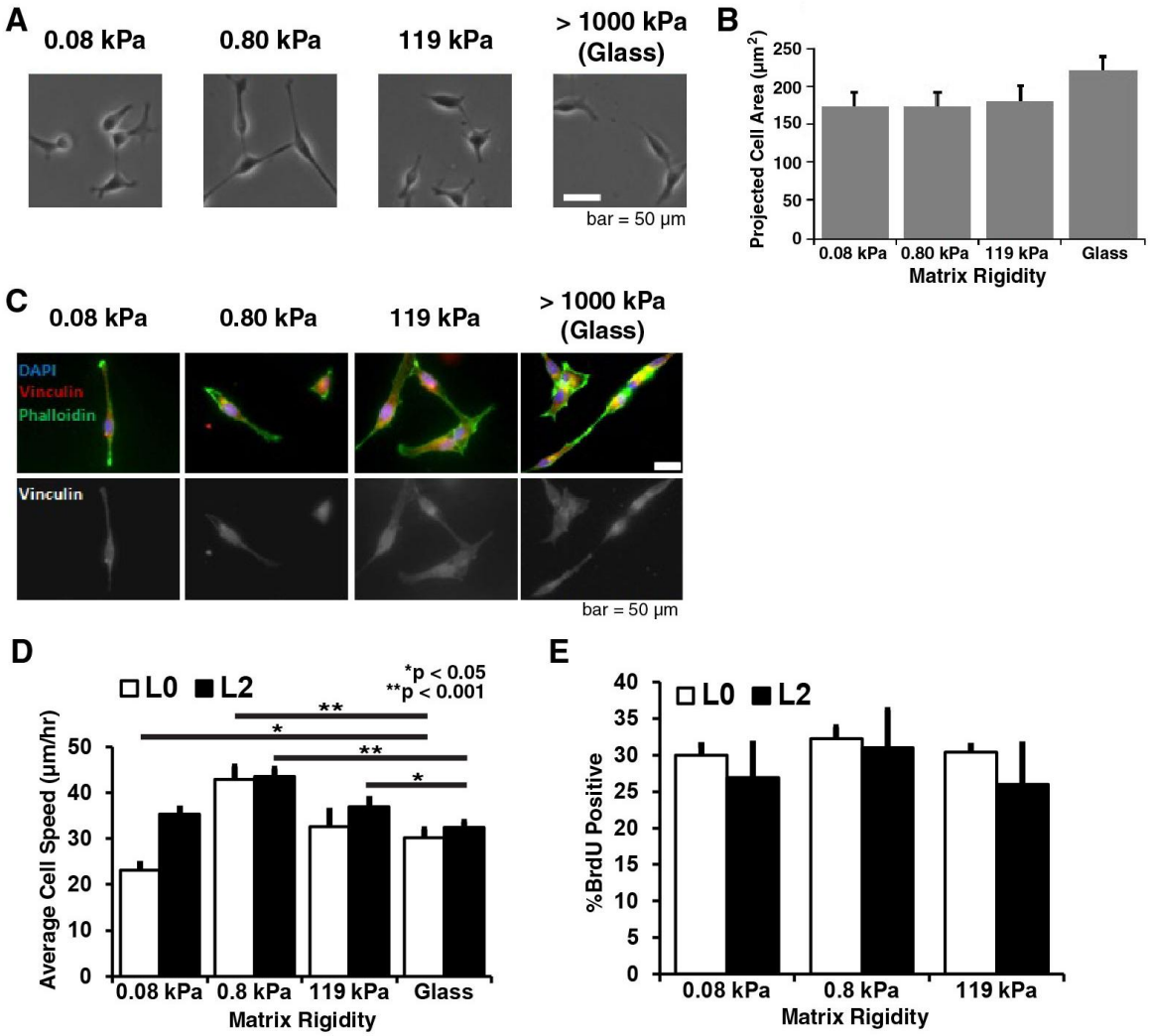


**Figure 2.2: TICs can spread, migrate, and proliferate on soft and stiff 2-D ECMs.** (A) effect of ECM stiffness on cell spreading. GBM TICs were cultured on laminin-coated polyacrylamide matrices, with stiffnesses ranging from 0.08 kPa to 119 kPa, and on laminin-coated glass. Phase contrast imaging reveals that GBM TICs can spread on ECMs of all stiffnesses. (B) quantification of projected cell area shows that ECM rigidity does not regulate L2 TIC spreading area. $n = 20$ cells (pooled from at least three technical and three biologic experiments) for all conditions. L0 TICs (not shown) exhibited qualitatively similar data. (C) GBM TICs do not form prominent stress fibers or focal adhesions on stiff ECMs. Cells were fixed and stained for the focal adhesion marker vinculin (red), F-actin (green), and nuclear DNA (blue). (D) effect of ECM stiffness on cell motility. Time-lapse phase contrast imaging of random cell motility over 8 to 12 hours indicate that the migration speed depends very weakly on ECM stiffness, with a modest optimum at 0.8 kPa. *, $P < 0.05$ and **, $P < 0.001$ relative to glass; $n > 80$ cells for all conditions. (E) effect of ECM stiffness on cell proliferation. Cells were incubated with bromodeoxyuridine (BrdUrd) for 45 minutes and stained with 7AAD before analysis by flow cytometry. Plots show sample means with SE. $n > 3$ independent experiments for all conditions.

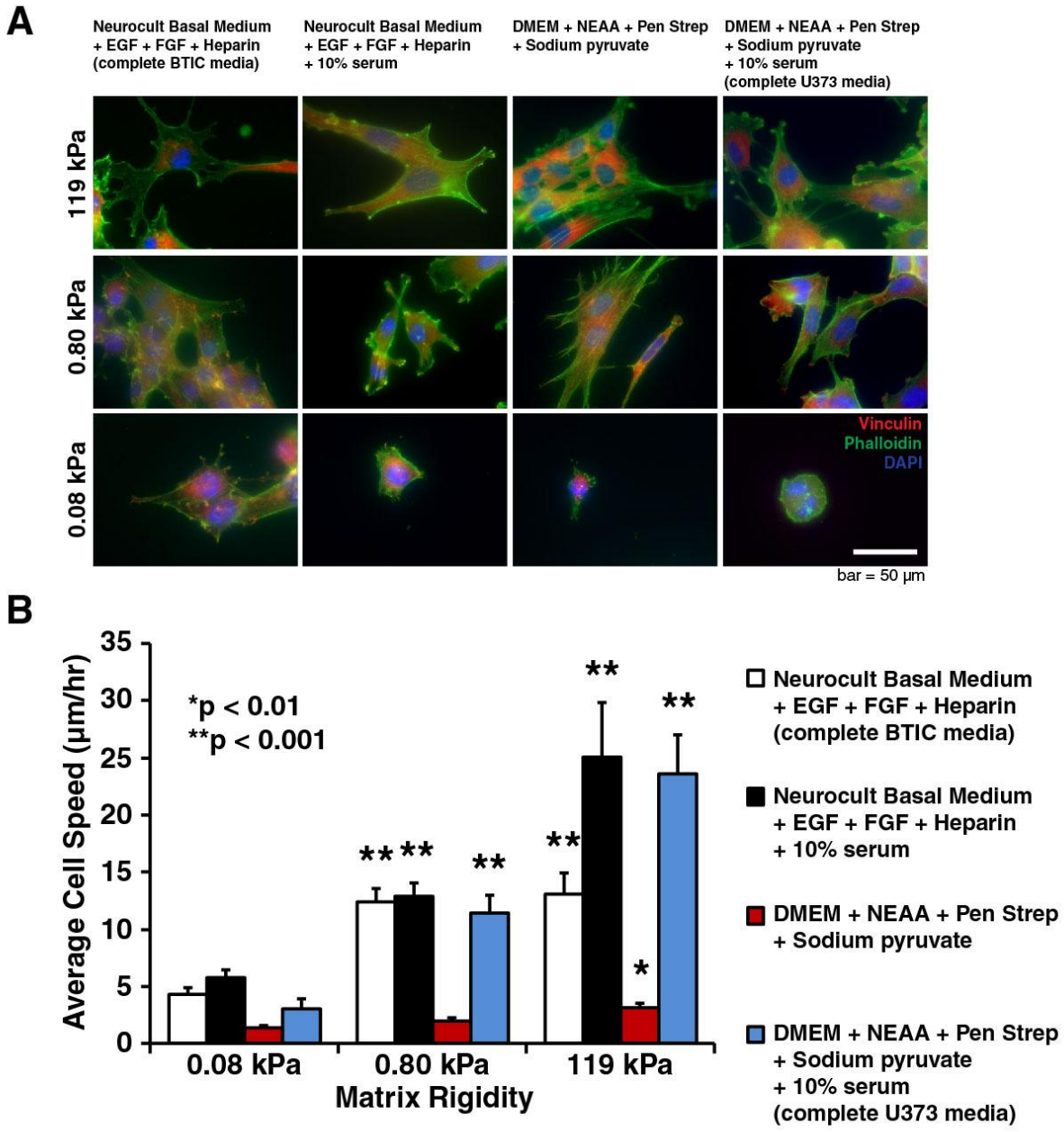


**Figure 2.S1: Lack of serum does not render continuous GBM cell line U373-MG insensitive to matrix stiffness.** (A) GBM continuous cell line U373-MG continues to exhibit sensitivity to ECM stiffness with or without addition of serum in the culture medium. Epifluorescence images of U373-MG cells show spread cells on stiff ECMs and rounded cells on soft ECMs irrespective of neurobasal or DMEM-based medium conditions. (B) U373-MG cells migrate at higher speeds on stiff ECMs in serum-free media. Measurement of U373-MG motility in various media conditions demonstrate that even in the absence of serum, cells migrate faster on stiff ECMs than soft ECMs. n > 30 per condition.

### 2.4.3. Myosin II-dependent contractility restricts rigidity-dependent spreading, motility, and invasion

Previously, we had shown that myosin II-dependent contractility is required for GBM tumor cells to sense ECM rigidity, in as much as pharmacologic inhibition of myosin rescues spreading and motility on compliant ECMs (41). This observation is consistent with a model in which cells must exert traction forces through myosin motors to deform the ECM and sample local stiffness (42,88). We therefore hypothesized that the ability of GBM TICs to evade motility limitations imposed by soft ECMs derives from insufficient generation of myosin-based contractile forces. Myosin-dependent cell contractility is activated by RhoA GTPase, which promotes myosin phosphorylation by activating Rho-associated kinase (ROCK; ref. 84). We thus performed gain-of-function studies in which we overexpressed a constitutively activated (CA) mutant of RhoA (Figure 2.3A) to determine whether increased contractility could restore suppression of motility on soft ECMs. Western blot analyses confirmed elevation of phosphorylated myosin light chain expression in the constitutively active GBM TIC lines (Figure 2.3B). To investigate the effect of CA RhoA on cellular mechanical properties, we used atomic force microscopy (AFM) to measure cell elasticity (Figure 2.3C). We found that transduction with CA RhoA conserved cell stiffness for L0 while pushing the observed stiffness range to higher values and significantly increased cell stiffness for L2 relative to control GBM TICs transduced with the control empty vector.

Expression of CA RhoA remarkably restored sensitivity to ECM stiffness, with CA RhoA GBM TICs significantly rounding up on soft ECMs and spreading on stiff ECMs (Figure 2.3D and E; L2 CA RhoA GBM TICs shown, with L0 CA RhoA GBM TICs yielding similar results). In addition, CA RhoA strongly retarded GBM TIC motility on soft ECMs compared with stiff ECMs (Figure 2.3F). Notably, GBM TIC proliferation (Figure 2.3G) and the universally positive expression of nestin and SOX2 (Figure 2.3H) remained relatively insensitive to ECM rigidity. In addition, both control and CA RhoA TICs could still form neurospheres (Figure 2.3I and J), which is a predictor of glioma tumor progression and is associated with poor clinical outcome (89). Altogether, these data confirm that constitutive activation of RhoA does not compromise GBM TIC self-renewal properties.

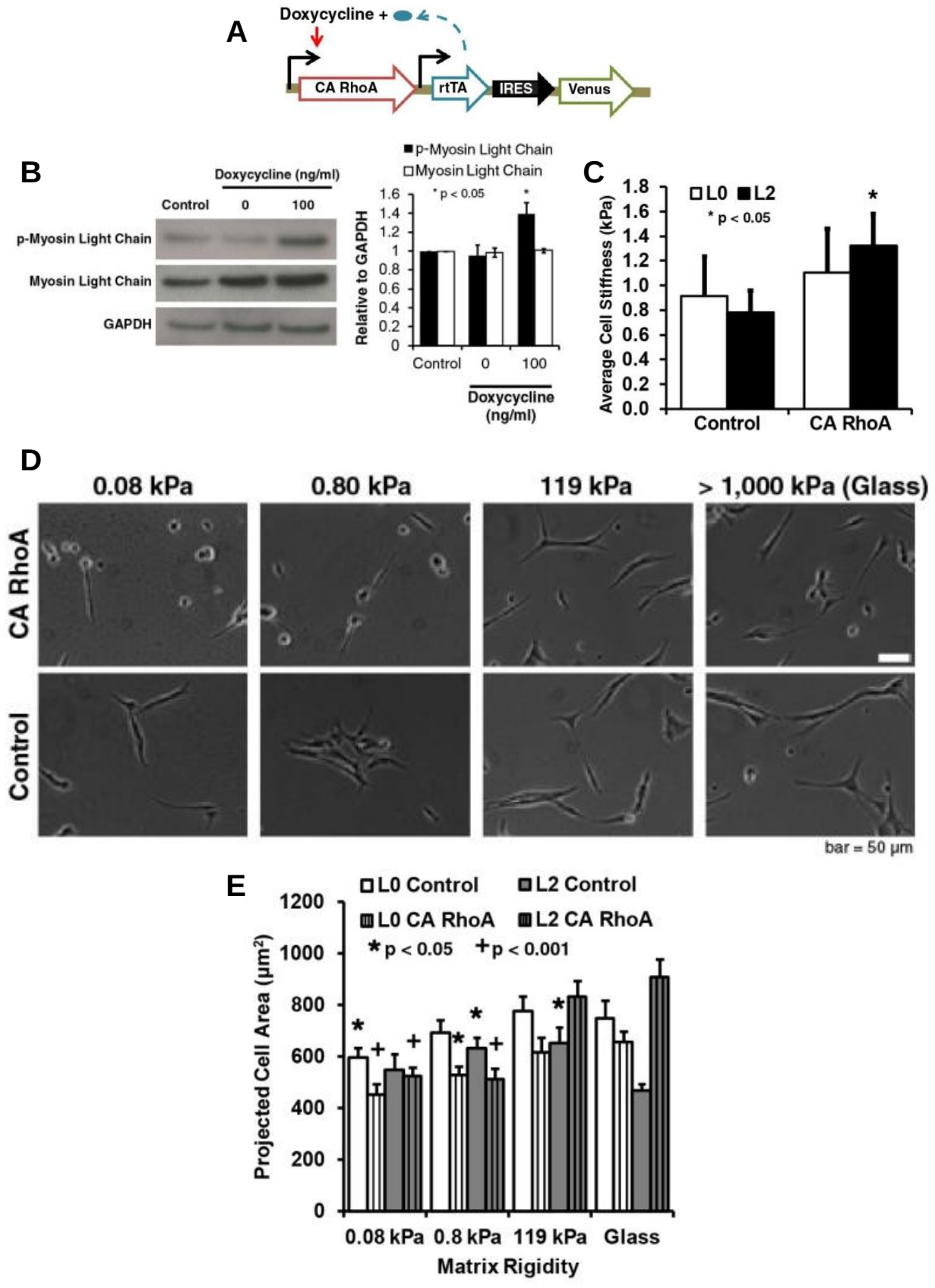
A
Doxycycline +
CA RhoA
rtTA
IRES
Venus
B
Doxycycline (ng/ml)
Control
0
100
p-Myosin Light Chain
Myosin Light Chain
GAPDH
p-Myosin Light Chain
Myosin Light Chain
* p < 0.05
Relative to GAPDH
Control
0
100
Doxycycline (ng/ml)
C
L0
L2
* p < 0.05
Average Cell Stiffness (kPa)
Control
CA RhoA
D
0.08 kPa
0.80 kPa
119 kPa
> 1,000 kPa (Glass)
CA RhoA
Control
bar = 50 μm
E
L0 Control
L2 Control
L0 CA RhoA
L2 CA RhoA
* p < 0.05
+ p < 0.001
Projected Cell Area (μm²)
0.08 kPa
0.8 kPa
119 kPa
Glass
Matrix Rigidity

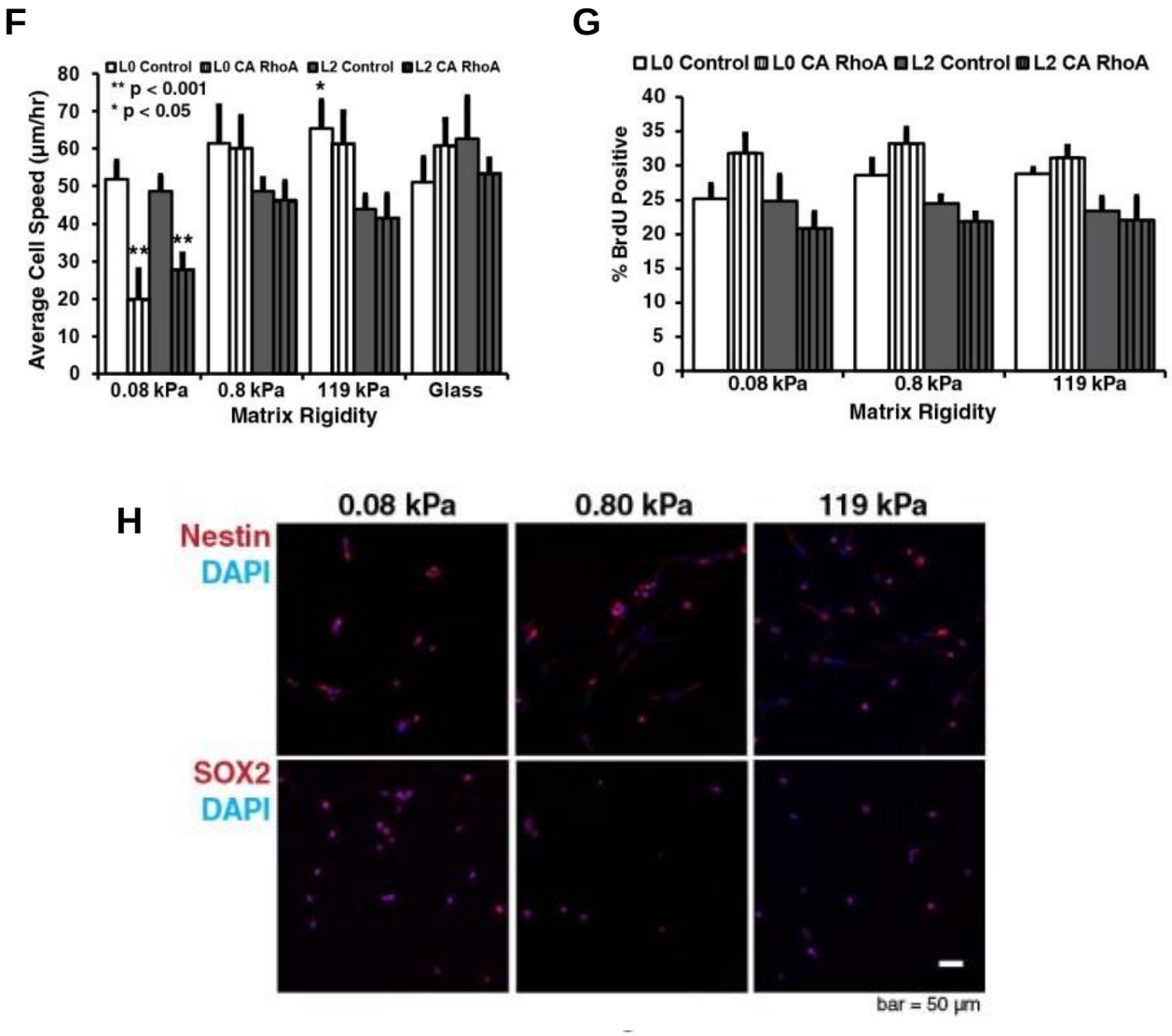
F
L0 Control
L0 CA RhoA
L2 Control
L2 CA RhoA
** p < 0.001
* p < 0.05
Average Cell Speed (μm/hr)
0.08 kPa
0.8 kPa
119 kPa
Glass
Matrix Rigidity
G
L0 Control
L0 CA RhoA
L2 Control
L2 CA RhoA
% BrdU Positive
0.08 kPa
0.8 kPa
119 kPa
Matrix Rigidity
H
0.08 kPa
0.80 kPa
119 kPa
Nestin
DAPI
SOX2
DAPI
bar = 50 μm
I
L0
L2
*p < 0.001
Sphere Forming Frequency
Control
CA RhoA
J
L0
L2
*p < 0.001
+p < 0.05
Relative Sphere Size
Control
CA RhoA

**Figure 2.3: Increased Rho GTPase activation leads to stiffness-dependent spreading and motility.** (A) genetic strategy for inducible activation of contractility. A constitutively active (CA) mutant of RhoA (or CA ROCK/CA MLCK as noted) was placed under the control of a doxycycline-inducible promoter, placed into a lentiviral vector, and used to transduce GBM TICs to yield stable cells lines. (B) RhoA induction increases myosin light chain phosphorylation. Western blot analysis confirms that induction of CA RhoA increases myosin light chain phosphorylation relative to control cells transduced with an empty vector. Data shown are for the L0 TIC line. $n = 3$ independent experiments. (C) CA RhoA preserves or enhances cell stiffness. AFM measurements reveal that overexpression of CA RhoA preserves mean cell stiffness in L0 cells (while pushing the range of observed stiffness values to higher values) and increases mean cell stiffness in L2 cells, consistent with an increase in cell contractility. $n = 10$ to 20 cells pooled from at least three biologic and technical replicates. (D) CA RhoA restores ECM stiffness-dependent spreading. Phase contrast imaging reveals that overexpression of CA RhoA produces cell rounding on soft ECMs, in contrast with control-transduced cells, which spread on ECMs spanning the entire range of stiffness. (E) quantification of projected cell area shows that CA RhoA rescues stiffness-dependent cell spreading, with significantly decreased spread area for CA RhoA TIC on soft ECMs. *, $P < 0.05$ and $^{+}$, $P < 0.001$ relative to glass. $n = 30$ cells (pooled from at least three technical and three biologic experiments) for all conditions. (F) CA RhoA rescues stiffness-dependent cell motility. Time-lapse phase contrast imaging of random cell motility over 8 to 12 hours shows significantly decreased motility of these cells on soft ECMs relative to stiff ECMs. *, $P < 0.05$ and **, $P < 0.001$ relative to glass. $n = 30$ cells for all conditions. (G) CA RhoA does not alter cell proliferation. Cells were incubated with bromodeoxyuridine (BrdUrd) for 45 minutes and stained with 7AAD before analysis by flow cytometry. The data reveal that overexpression of CA RhoA neither produces statistically significant changes in proliferation for any given ECM stiffness nor does it render proliferation sensitive to ECM stiffness. $n = 3$ independent experiments. (H) CA RhoA TICs express the stem cell markers nestin (top row; 100% positive) and SOX2 (bottom row; 100% positive) on all ECM stiffnesses. (I) CA RhoA does not compromise the ability of TICs to form neurospheres. *, $P < 0.001$ relative to control, $n = 384$ TICs. (J) quantification of neurosphere size for L0 and L2 cells as a function of RhoA expression. *, $P < 0.001$ and $^{+}$, $P < 0.05$ relative to control, $n = \sim 1{,}500$ spheres for all conditions.

To verify that the observed increase in contractility is due to myosin activation per se as opposed to other downstream effects of RhoA activation, we treated CA RhoA GBM TICs with the myosin II ATPase inhibitor blebbistatin, which rescued spreading of CA RhoA TICs on the softest ECM (Figure 2.4A). Consistent with this finding, treatment with blebbistatin did not yield systematic dependences of spreading area (Figure 2.4B) or migration speed (Figure 2.4C) as a function of matrix stiffness for either control or RhoA TICs. To investigate potential effects of blebbistatin on growth, we measured TIC proliferation (Figure 2.4D) and viability (Figure 2.4E) as a function of ECM stiffness and CA RhoA expression, which did not reveal systematic effects of the drug. Given the demonstrated importance of the myosin II isoforms A, B, and C to glioma invasion (63,90), we also measured isoform expression as a function of ECM stiffness and CA RhoA status. Western blot analyses (Figure 2.4F and G) revealed that TICs express all three isoforms under all stiffnesses and in the presence or absence of CA RhoA induction. To confirm and quantify these results, we obtained mass spectrometry data (Figure 2.4H), which revealed myosin IIA to be the dominant isoform and the relative ratio of isoforms A, B, and C to be largely unchanged across all conditions. Thus, stiffness- and RhoA-mediated effects in this system do not appear to be a consequence of changes in the myosin II isoform ratio.

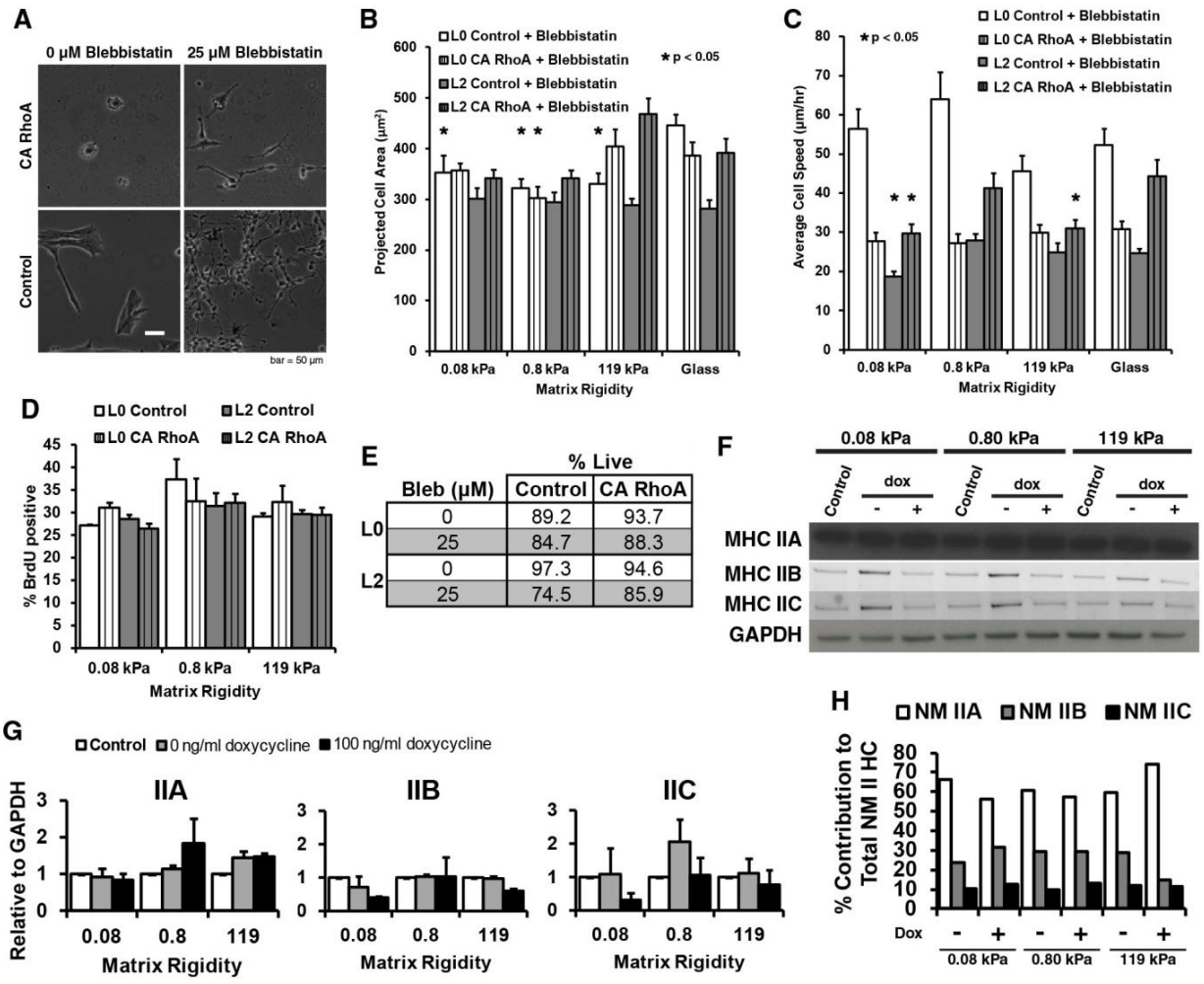


**Figure 2.4: Nonmuscle myosin II regulates TIC mechanosensitivity.** (A) CA RhoA-mediated suppression of cell spreading can be rescued with pharmacologic inhibition of myosin-II. Addition of 25 μmol/L of blebbistatin results in spreading of CA RhoA GBM TICs on soft ECMs, similar to the control GBM TICs. (B) quantification of projected cell area shows that addition of blebbistatin reverses CA RhoA effects and caused CA RhoA TICs to spread on soft ECMs. *, $P < 0.05$ relative to glass; $n = 30$ cells pooled from at least three technical and three biologic experiments for all conditions. (C) quantification of blebbistatin effects on cell migration speed. Time-lapse phase contrast imaging of random cell motility was conducted over 8 to 12 hours. *, $P < 0.05$ relative to glass; $n = 30$ cells for all conditions. (D) CA RhoA TIC proliferation is not systemically altered by addition of blebbistatin. Cells were incubated with bromodeoxyuridine (BrdUrd) for 45 minutes and stained with 7AAD before analysis by flow cytometry. Plots show sample means with SE. $n = 3$ independent experiments for all conditions. (E) live/dead assay with propidium iodide staining shows that TICs remain viable in the presence of blebbistatin. (F) Western blot analysis of myosin II heavy chain isoforms A, B, and C show that control and CA RhoA TICs express all three isoforms on all ECM stiffnesses (L2 shown; L0 had similar results). (G) quantification of Western blot data; $n > 2$ independent experiments. (H) relative levels of myosin II heavy chain isoforms measured by LC/MS-MS. $n = 2$ experiments per condition.

To test the generality of the effect of increased myosin activity on cell migration, we developed additional GBM TIC lines overexpressing CA mutants of the contractile activators ROCK1 (Figure 2.5A) and myosin light chain kinase (MLCK; Figure 2.5B), the latter of which activates myosin through an orthogonal, RhoA-independent mechanism. Indeed, overexpression of either molecule produced highly rigidity-dependent motility, with soft ECMs strongly suppressing motility. Thus, suppression of motility on these highly compliant ECMs is consistently associated with generation of high contractile forces against the ECM.

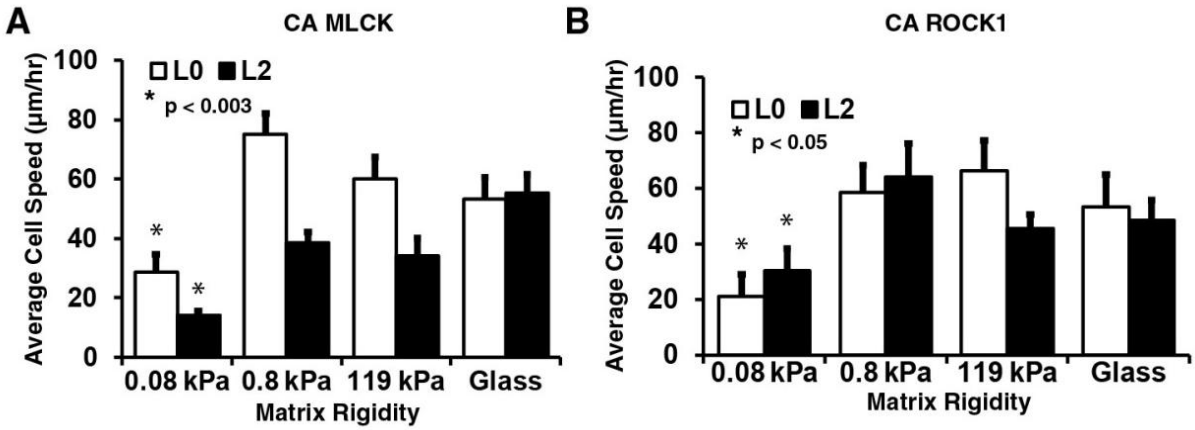


**Figure 2.5: TICs overexpressing other contractile activators also exhibit stiffness-dependent motility and spreading.** Lentiviral transduction of L0 TICs with CA MLCK (A) and CA ROCK1 (B) resulted in increased average cell speed on stiff ECMs compared with soft ECMs and in restored mechanosensitive migration speed. *, $P < 0.003$ relative to glass. $n$ = 10-20 cells pooled from at least three biologic and technical replicates per condition.

To determine whether activation of contractile signaling could also limit motility in three-dimensional ECMs that better capture steric and architectural features of tissue ECM, we performed spheroid invasion assays in soft collagen I gels (Figure 2.6A). Consistent with our 2-D migration studies, RhoA activation almost completely abrogated invasion relative to control cells transduced with an empty vector. RhoA activation also produced a 39% reduction in migration through laminin-coated 3-μm pore size Transwell inserts (Figure 2.6B). Notably, treatment ofTICs with BMP-4 also significantly reduced invasion in both cell lines (Figure 2.S2C).

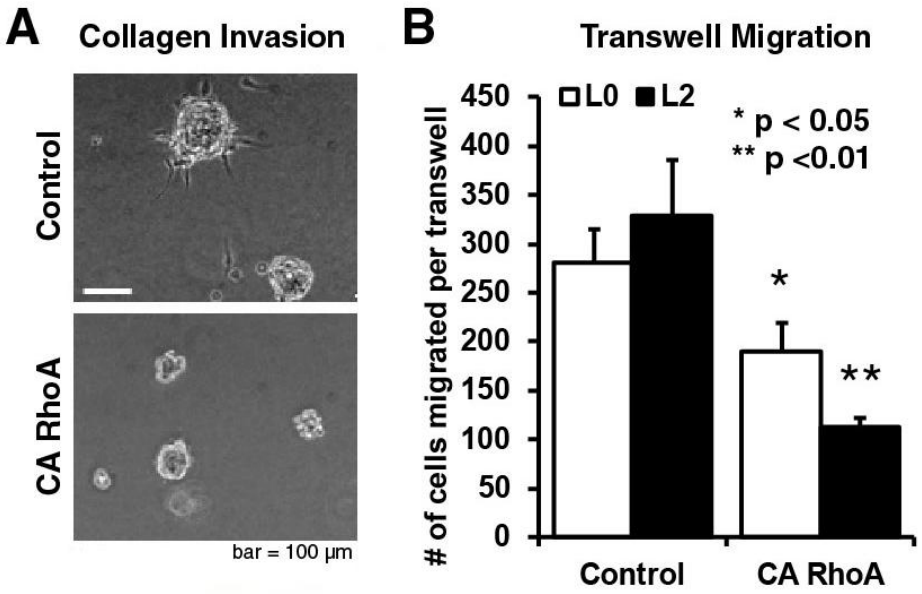


**Figure 2.6: Increased Rho GTPase activation limits invasion and motility in 3-D.** (A) CA RhoA prevents GBM TICs from invading 3D collagen ECMs. Images depict spheroids formed from CA RhoA or control GBM TICs, implanted in 1.0 mg/mL collagen gels, and captured by phase contrast imaging 3 days later. n > 8 spheroids per condition for all conditions. (B) CA RhoA reduces Transwell migration of GBM TICs. Transwell inserts were coated with laminin, and CA RhoA and control cells were allowed to migrate through pores for 24 hours before fixation. A 2X gradient of soluble EGF was used to drive chemotaxis through the pores, and the total number of cells migrated per Transwell was counted. Data shown are for the L2 TIC line; L0 TICs exhibited qualitatively similar data.

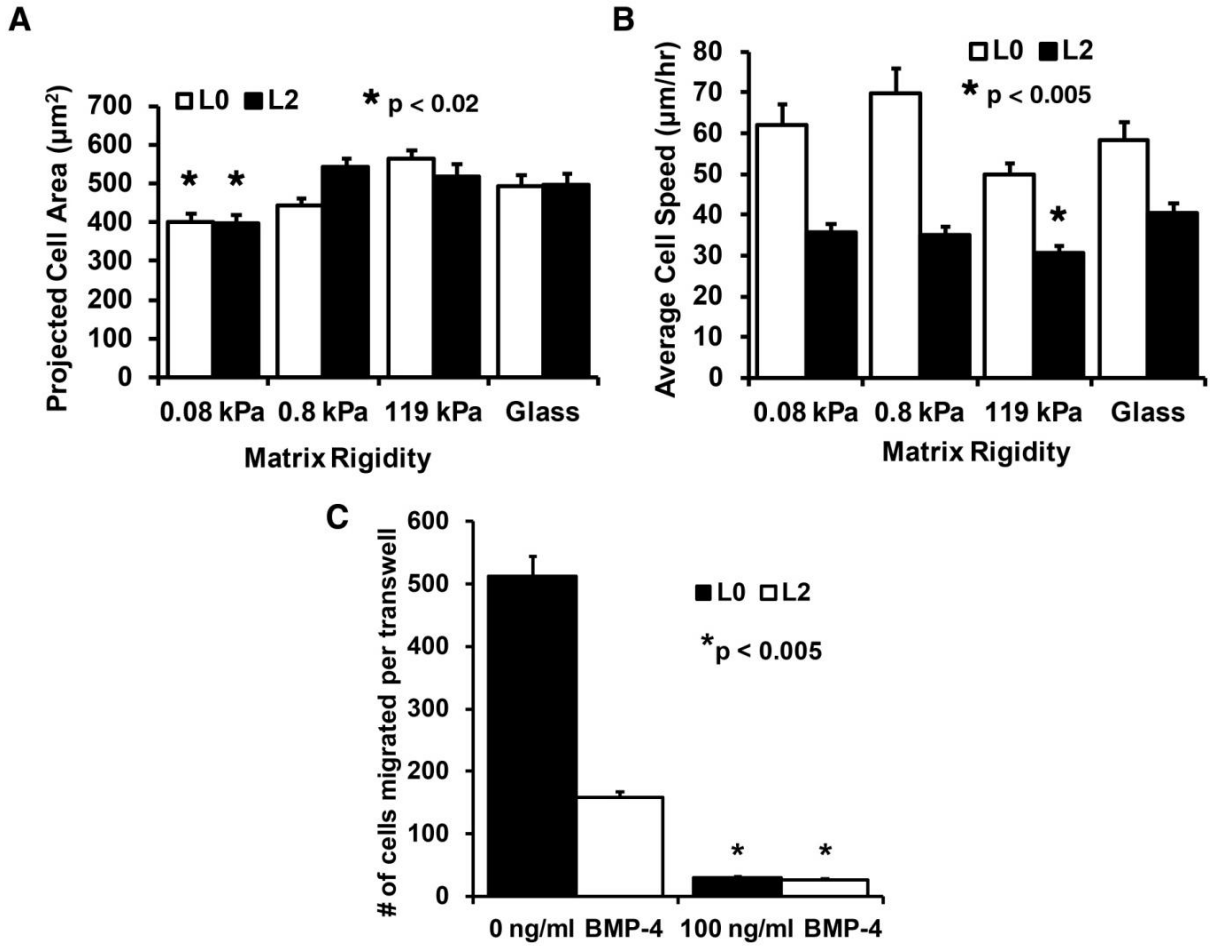


**Figure 2.S2: BMP4-induced differentiation alters tumor-initiating cell spread area, but not motility.** (A) Effect of BMP4 on ECM stiffness-dependent spreading. BMP4 was added to TICs for 48 hrs to induce differentiation; quantification of projected cell area shows that BMP4 treated TICs have significantly reduced cell spread area on soft ECMs. *$p<0.02$ relative to glass, n=30 cells pooled from at least three technical and three biological experiments for all conditions. (B) Effect of BMP4 on migration speed. Time-lapse phase contrast imaging of random cell motility over 8-12 hours show that BMP4 differentiated TICs do not exhibit significant differences in motility across all ECM stiffnesses. *$p<0.005$, n=30 cells for all conditions. (C) BMP-4 differentiation reduces migration of GBM TICs. Transwell inserts were coated with laminin, and TICs were allowed to migrate through pores for 24 hours before fixation. A 2X gradient of soluble EGF was used to drive chemotaxis through the pores, and the total number of cells migrated per Transwell was counted.

### 2.4.4 Increased cellular contractility extends survival time in an orthotopic mouse model

Finally, to test whether contractility-mediated restriction of GBM TIC motility could reduce tumor invasion and initiation *in vivo*, we compared the tumorigenicity of CA RhoA with control GBM TICs in a mouse orthotopic xenograft model. We intracranially injected GBM TICs transduced with either CA RhoA or an empty vector into immunocompromised (NSG) mice and followed each cohort until death (Figure 2.7A). Remarkably, RhoA activation prolonged survival time by 30% (Figure 2.7B). IHC analysis further revealed that tumors seeded by CA RhoA GBM TICs had reduced invasion capacity and highly circumscribed growth patterns (Figure 2.7C), whereas control GBM TICs diffusely spread throughout both hemispheres and generated a secondary tumor in the contralateral hemisphere, consistent with human GBMs (Figure 2.7D, i–iii, v–vii). Moreover, although both CA RhoA and control GBM TICs were able to form tumors *in vivo*, only tumors derived from the control GBM TICs exhibited all of the defining morphological characteristics of GBM: pseudo-palisading necrosis, nest-like formations, angiogenesis, and mitotic figures. Notably, both control and CA RhoA GBM TICs also continued to express nestin (Figure 2.7D, iv, viii), illustrating retention of an important TIC marker throughout the growth and invasion process. Quantification of tumor cross-sectional area confirmed that the area occupied by CA RhoA TIC-induced tumors is >3.5-fold lower than control TIC-induced tumors (Figure 2.7E). To verify that the difference in tumor occupancy was not a result of cellular proliferation, tissue sections were stained with the antibody Ki-67 (Figure 2.7F). We found no difference in proliferation between control and CA RhoA GBM TICs, lending further support to the notion that the reduction in tumor invasion more likely stemmed from limited migration than altered cell division.

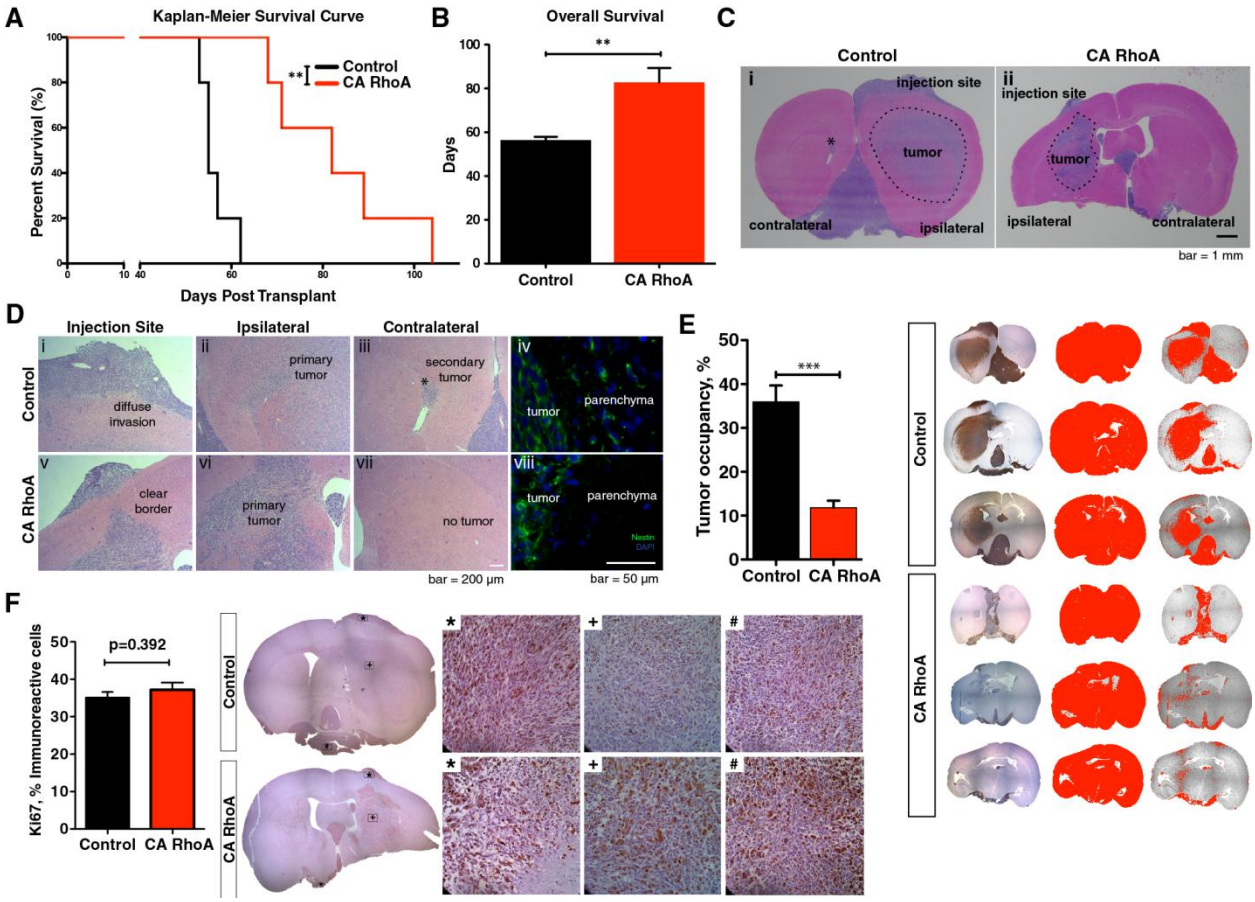


**Figure 2.7: Constitutive activation of RhoA in GBM TICs extends survival time and reduces tumor invasion in an orthotopic xenograft model.** (A) mice orthotopically implanted with L0 CA RhoA GBM TICs live significantly longer than mice implanted with L0 control TICs. Eight-week-old NSG mice were implanted intracranially with 200,000 cells. Mice were treated daily with doxycycline (625 mg/kg) 4 days post implant until endpoint. **, $P = 0.0018$, log-rank test. $n = 5$ mice per condition. (B) CA RhoA results in a 30% increase in overall mouse survival. **, $P = 0.0042$, *t* test. (C) tumors formed from L0 CA RhoA GBM TICs do not infiltrate brain tissue as extensively as L0 control TICs. Hematoxylin and eosin stain shows (i) a large area of infiltration and secondary tumor formation (*) in mice implanted with L0 control TICs; and (ii) a defined area of infiltration with clear borders and no secondary tumor formation in mice implanted with L0 CA RhoA GBM TICs. (D) CA RhoA reduces diffuse invasion in GBM. Hematoxylin and eosin (i, v) and human nestin stains (iv, viii) reveal a clear border between CA RhoA tumors and the parenchyma whereas control GBM TICs infiltrate readily. Ipsilateral (ii) and contralateral (vi) hemisphere hematoxylin and eosin stains show secondary tumor formation (*) for control cells and not for CA RhoA cells. (E) human GBM cells were identified using anti-human Nestin antibody and visualized using the ABC-Elite peroxidase method (Vector Laboratories). Counterstaining of the nuclei was performed using hematoxylin. Analysis of cross-sectional area shows significantly decreased tumor occupancy for mice brains implanted with L0 CA RhoA TICs compared with L0 control TICs. Graph shows average ± SE over 5 to 8 sections per group. ***, $P < 0.0001$. (F) Ki-67 staining and quantification show no difference in cell proliferation across multiple regions in control and CA RhoA GBM TICs.

## 2.5 Discussion

Mechanical signals encoded in the ECM are increasingly recognized as important regulators of tumor progression (68,91,92). It has also been shown that continuous culture models of GBM require myosin II and its upstream regulators to sense and respond to ECM rigidity (41,43,65,93). However, it has remained unclear whether these principles apply to primary TICs, or whether manipulation of the mechanosensing machinery can influence tumor initiation and progression *in vivo*. Here, we have addressed these questions by elucidating connections between mechanosensitivity *in vitro*, activation of contractile signals, and tumor progression and survival *in vivo*. We discovered that primary GBM TICs can evade limits on spreading and motility normally imposed by compliant matrices by generating low contractile forces. Constitutive activation of myosin II increased GBM TIC contractility, severely restricted GBM TIC motility on compliant ECMs and limited invasion through three-dimensional matrices. Moreover, mice orthotopically implanted with GBM TICs in which contractile signaling had been activated developed smaller and less invasive tumors *in vivo* relative to control, and exhibited 30% increased overall survival. These findings provide strong support for the notion that GBM can be regarded as a disease of cell migration, and that targeting signals that influence this process *in vitro* can also influence disease progression *in vivo*.

Several studies have explored regulatory roles of the Rho GTPases and myosin II in GBM tumor progression, although different experimental systems have produced a somewhat equivocal view of whether activation of these pathways promotes or suppresses tumorigenesis. For example, pharmacologic and/or genetic suppression of myosin II has been shown to reduce glioma invasion in xenograft, genetic, and slice culture models, which has been attributed to the importance of myosin II in squeezing the nucleus through tight tissue spaces during invasion (63,90). Consistent with this finding, simultaneous activation of Rac and RhoA has been found to increase the invasive capacity of GBM TICs (94). In contrast, another study revealed that hyperactivation of Rac1 and Cdc42 through silencing of β8 integrin diminishes GBM invasion with concomitant increases in tumor volume in a mouse xenograft model (95). Although these studies may appear to be mutually contradictory, they can be reconciled by considering the notion that activation of these pathways is likely to be highly dynamic and regulated both within and across tumor cells, as well as significantly variable from one physical microenvironment to another. This may give rise to highly nonlinear phenotypic effects that may defy easy prediction. For example, although perinuclear myosin II activation may be critical to nuclear deformation during migration, myosin activation can limit the cytoskeletal plasticity needed for process extension (84). Indeed, recent *in vivo* florescence resonance energy transfer studies demonstrate that Rho, Rac, and Cdc42 activation vary dramatically in glioma tumor cells as they invade the brain, with different anatomical modes of invasion recruiting different molecular machinery (96). Constitutive activation of myosin and its activators, as we do in this study, would override these regulatory effects and prevent tumor cells from attenuating and enhancing contractility as needed for productive migration. Moreover, Shin and colleagues (97) recently showed that inhibition of myosin II in hematopoietic stem and progenitor cells preferentially enriched the stem cell population, which is broadly consistent with our observations that TICs evade restrictions on adhesion and proliferation normally imposed by highly compliant ECMs. Nonetheless, it is important to note that RhoA has diverse functions and that our *in vivo* results may not derive exclusively from altered mechanotransductive signaling. Additional *in vivo* genetic and

pharmacological gain- and loss-of-function studies targeting other proteins that enhance and suppress contractility should help to clarify this issue.

Although the patient-derived L0 and L2 TIC lines used here behaved in a broadly similar fashion across the vast majority of our assays, they did differ in some respects, most notably neurosphere formation frequency and size (Figure 2.3I and J). Both lines were derived from classical-subtype GBM tumors but were isolated from different patients and thus would be expected to exhibit some phenomenological differences in specific assays. In addition, neurosphere-forming properties are expected to be a complex function of cell–cell adhesion, proliferation rate, cell contractility, and other factors, small perturbations in any one of which could unpredictably alter the endpoint readout.

Interestingly, while we find that activation of contractile signaling reduces motility, invasion, and tissue infiltration, neither RhoA activation nor ECM stiffness significantly influences proliferation, expression of TIC markers, or differentiation potential. This would suggest that these manipulations do not exert a significant selective effect, which is consistent with our finding that the slowest-cycling (and most highly tumorigenic) subpopulation is preserved across all matrix rigidities.

Finally, our study points to the potential importance of the cell–matrix mechanosensing machinery in GBM TIC physiology. A number of matrix adhesion-related molecules have been identified as GBM TIC markers, including α6 integrin (32), CD44/moesin (38), and laminin α2 (98). In addition to being correlative predictors of tumor-initiating potential, these molecules may play important functional roles that directly promote tumor growth and invasion. For example, pharmacologic disruption of the CD44/moesin interface strongly reduces GBM TIC proliferation (38), and inhibition of integrin α6 promotes tumor latency and survival (32). Complementary to these studies, our work demonstrates that GBM TICs can evade ECM stiffness-induced suppression of cell motility, analogous to their widely observed resistance to radiation and chemotherapeutic inputs. We hypothesize that tumor cells making up the bulk of the tumor may have relatively high contractility, and are thus prevented by the soft microenvironment from invading into the parenchyma. Previous cortical stiffness measurements of the continuous cell line U373-MG average at 2 kPa (84) which is more than two times higher than the value of our GBM TIC stiffness measurement of 0.8 kPa (Figure 2.3C). GBM TICs seem to have adapted to the soft environment by generating lower contractility and can thus aggressively invade through brain tissue to initiate new tumors. One method to override this GBM TIC adaptation is to hyperactivate the underlying mechanotransductive actuation mechanisms, which renders GBM TICs susceptible to soft matrix suppression both *in vitro* and *in vivo*. In the future, it would be valuable to systematically compare sensitivity to ECM stiffness and RhoA activation across matched, explanted tumor subpopulations at well-defined stages of differentiation, and across cultured TICs at various times after morphogen-induced differentiation. It would also be highly informative to repeat these studies with a panel of TICs derived from all transcriptional subtypes of GBM to determine whether these phenotypes are specific to classical GBMs or a more generic feature of TICs. Collectively, previous studies and our findings raise the exciting possibility that mechanisms through which GBM TICs physically engage the ECM can serve as a novel set of druggable targets.

## 2.6 Acknowledgements

The authors thank the following individuals: Dr. David Schaffer and Dr. Song Li for sharing equipment and reagents for Western blot and immunohistochemistry analysis; Dr. Robert Adelstein, Dr. Xuefei Ma, and Dr. Antoine Smith at NIH for mass spectrometric analysis of myosin II isoforms; Hector Nolla for technical assistance with flow cytometry; Dr. Mary West and Dr. Pingping He for assistance with instrumentation in the CIRM/QB3 Stem Cell Shared Facility; and Kevin Yamauchi and Dr. Amy Herr at UC Berkeley for use of the Typhoon FLA 9500 biomolecular imager for Western blot visualization.

This work was supported by grants (to S. Kumar) from the NIH (1DP2OD004213, Director's New Innovator Award; 1U54CA143836, Physical Sciences Oncology Center Grant; 1R21EB016359; 1R21CA174573), the W. M. Keck Foundation, and a Samsung Global Research Outreach Program. S.Y. Wong was supported by a California Institute for Regenerative Medicine pre-doctoral fellowship and a Cancer Research Coordinating Committee fellowship.

# Chapter 3: Concluding Remarks

This dissertation describes the application of technologies in the fields of bioengineering and stem cell biology to address fundamental questions in mechanobiology of glioma initiation and invasion. As discussed in Chapter 1, the identification and characterization of glioma TICs has been impactful to the field; however, tumor invasion also involves TIC interaction with its extracellular matrix, and so understanding matrix regulation of TICs may contribute to the development of effective therapies. The work presented in this dissertation demonstrates that the ECM and cellular architecture play a key role in regulating glioma TIC physiology, survival, and invasion in 2D and 3D culture systems as well as in a mouse model. This work has built upon previous glioma mechanobiology studies from within the lab and from others, and has laid the foundation for future research directions related to TIC characterization, tissue engineering, stem cell therapy for regenerative medicine applications, and importantly, targeted chemotherapy and gene therapy. In this chapter, I will summarize the results and significance of the preceding chapter, and briefly describe a promising ongoing collaboration that stemmed from this work.

## 3.1 Summary and Significance

In Chapter 2, we used 2D ECMs to study regulation of TIC motility, invasion, and proliferation by matrix mechanics. We found that, unlike other cell types, TICs were insensitive to changes in ECM stiffness, and their motility was not inhibited by soft ECMs (99). We then manipulated TIC contractility by overexpressing myosin activators, which restored mechanosensitivity and reduced 2D motility, particularly on highly compliant ECMs. Constitutive activation of RhoA GTPase also reduced 3D migration and invasion, further confirming the key role of contractility in regulation of TIC invasion and sensitivity to ECM stiffness. Lastly, we injected TICs in an orthotopic mouse model and found that RhoA activation reduces infiltration and significantly extends survival (Figure 3.1). Ongoing studies from other members of the Kumar Laboratory have subsequently explored related aspects of TIC invasive properties. For example, Jasmine Hughes is studying how other proteins in the contractility pathway, namely Rho-associated Kinase (ROCK) and myosin light chain kinase (MLCK), interact to regulate TIC invasion. George Lin and Dr. Joanna Bechtel-Dahl are studying the basis of TIC heterogeneity by using microfluidic systems to separate subpopulations for genomic and proteomic analyses. Collectively, our studies show that TICs have unique mechanosensory characteristics that allow them to override soft ECM cues that would otherwise limit invasion.

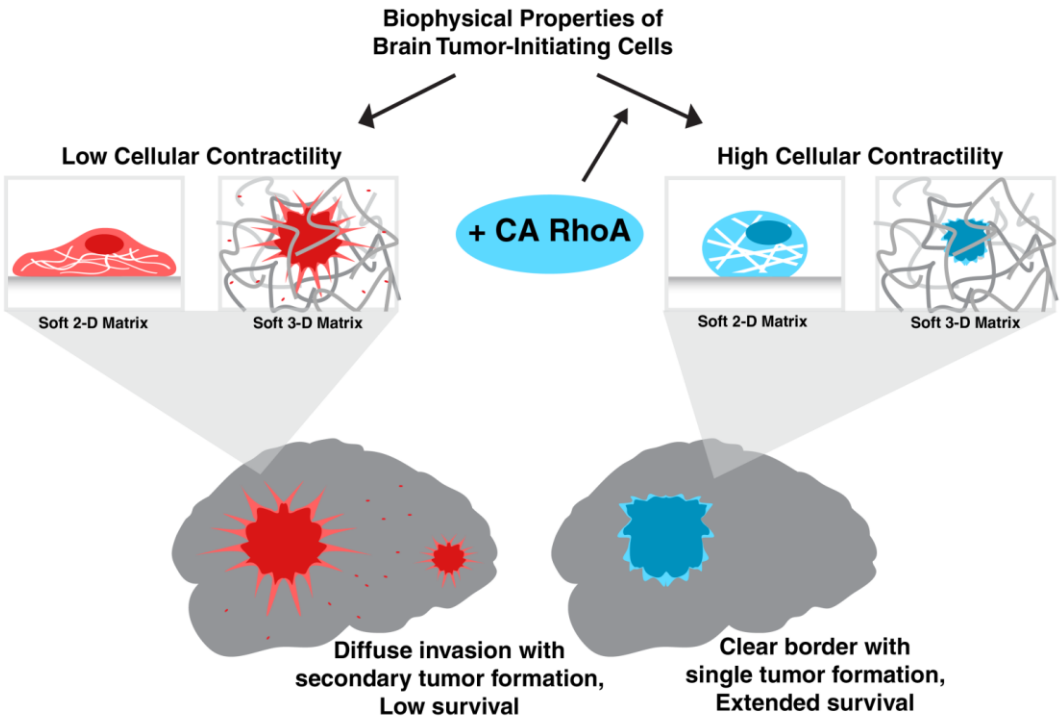


**Figure 3.1: Summary of TIC properties and experimental results.** *In vitro* 2D and 3D studies show that TIC mechanosensitivity can be rescued with upregulation of myosin activators, leading to reduced migration and invasion in soft ECMs. *In vivo* studies show that CA RhoA can reduce overall tumor occupancy and significantly extend survival in mice.

## 3.2 Future work and final thoughts

The results presented in the preceding chapter of this dissertation directly led to the development of a promising collaboration project with Jorge Santiago-Ortiz in the laboratory of Dr. David Schaffer.

### 3.2.1 Directed evolution of AAV to target glioma tumor-initiating cells

As presented in this dissertation and in studies conducted by others in the field, the existence and therapeutic resistance of TICs are believed to represent key barriers that undermine the effectiveness of traditional therapies for glioblastoma: surgery, radiation, and chemotherapy. Thus, development of therapeutics that specifically target TICs could give rise to more effective clinical responses and longer survival times. In collaboration with the Schaffer Laboratory, we seek to develop gene therapy strategies for GBM that are based on specific targeting of TICs.

It has been demonstrated in numerous studies that gene therapy can be successful and safe (100). Specifically, adeno-associated virus (AAV) vectors are relatively non-pathogenic; indeed, a large majority of the population is estimated to be seropositive for AAV antibodies, indicating prior

environmental exposure (101,102). Jorge has engineered an AAV vector in which we are using to optimize for strong tropism for TICs through several rounds of directed evolution, which involves generation of large AAV genetic libraries and iterative rounds of selection for improved function. To begin, we conducted three rounds of directed evolution *in vitro*. AAV libraries were added to adherently cultured TICs at an initial genomic MOI of 10,000, and then after seven days the cells were harvested and successful variants were recovered and amplified for the next round of evolution. The stringency of selection was increased by decreasing the genomic MOI to 1,000 in the second round and 100 in the third round of infection. The viral genomic titers of the recovered particles were then measured by PCR. These titers increased with each round, suggesting that the selection resulted in more infectious particles. These *in vitro* rounds of evolution resulted in identification of two promising variants that have some tropism to TICs - AAV3 and AAV6 (Figure 3.2). We then moved onto *in vivo* direct evolution. Non-obese diabetic/severe combined immunodeficient gamma (NSG) mice were orthotopically xenograted with TICs, and then after tumor development (21 days), animals were systemically injected with the AAV library. To track tumor development live using bioluminescence imaging, we stably transduced TICs to express a firefly luciferase gene (Figure 3.3). After six weeks - sufficient time for variants to be delivered to the tumor - brain tissue was harvested and successful variants were recovered and amplified for the next round. We have successfully completed one round of *in vivo* evolution and are conducting sequencing analysis.

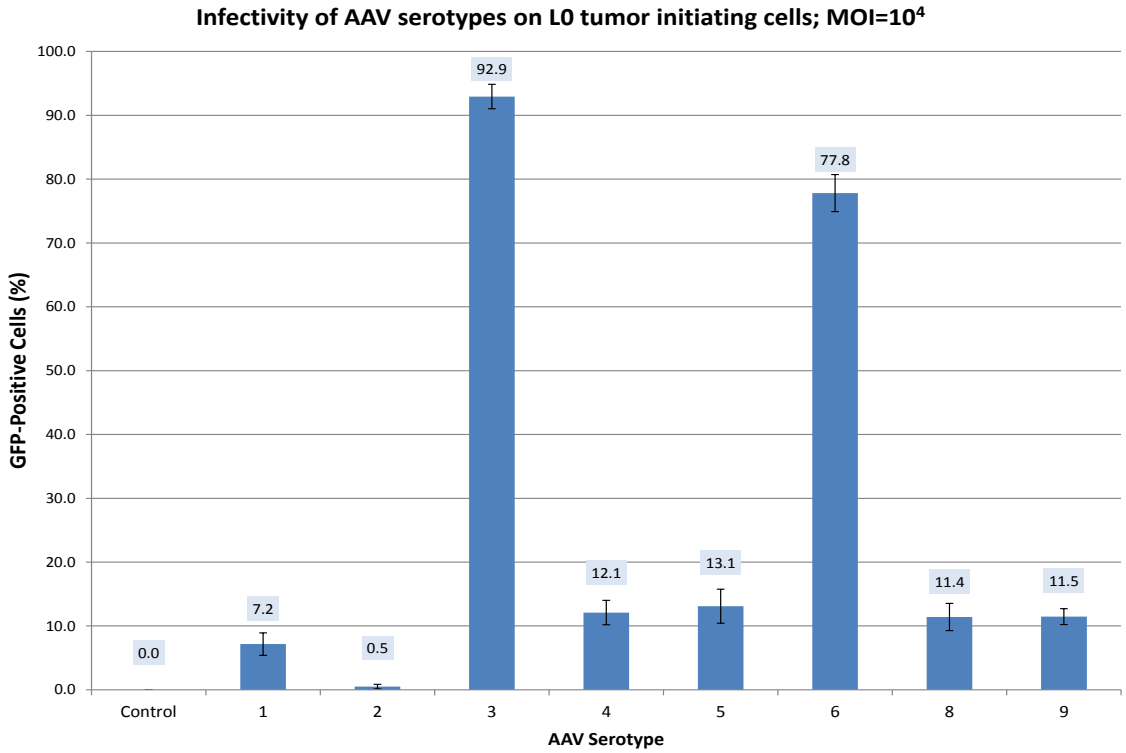


**Figure 3.2: Ratio of infectious to genomic MOI (X $10^5$) of natural AAV serotypes on TICs.** Cultured cells were transduced with vectors packaged with a self-complementary CMV-GFP cassette at a genomic MOI of 10,000 viral genomes/cell. The fraction of GFP-positive cells was quantified by flow cytometry 72 hours later. Data presented as mean ± SEM, n=3.

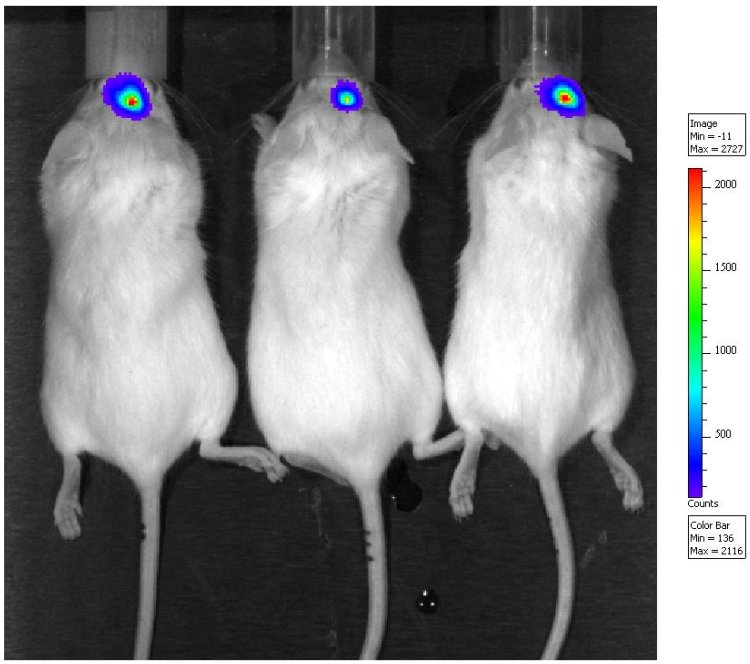


**Figure 3.3: Bioluminescence imaging of tumor-bearing mice after transplantation of luciferase-expressing TICs.** Image taken 7 minutes after luciferin administration 25 days after injection of TICs.

### 3.2.2 Final thoughts

The work presented in this dissertation has focused on understanding the properties of glioma TICs and their interactions with the surrounding tissue environment. Specifically, we studied effects of mechanotransductive signaling on TIC invasion and initiation using a variety of *in vitro* and *in vivo* approaches. Current therapies mainly target tumor cell proliferation. Although limiting tumor expansion through proliferation is very important and usually the first line of treatment, it is also essential to find therapies that limit tumor invasion. As I have shown in my work here (and in studies conducted by others), GBM is a disease of tumor cell invasion, and it is critical to develop therapies that can limit this invasion, which can result in significant reduction of tumor occupancy and increased survival time. In addition, after TICs migrate away from the primary tumor and as they invade through the surrounding tissue, they must find a place to stop and initiate a new tumor. A better understanding of how and why these events occur could be instrumental in developing effective combination therapies for GBM.

# References


1. Rouzier R, Perou CM, Symmans WF, Ibrahim N, Cristofanilli M, Anderson K, et al. Breast Cancer Molecular Subtypes Respond Differently to Preoperative Chemotherapy. Clin Cancer Res. 2005;11:5678–85.

2. Magee JA, Piskounova E, Morrison SJ. Cancer Stem Cells: Impact, Heterogeneity, and Uncertainty. Cancer Cell. 2012;21:283–96.

3. Banerjee S, Reis-Filho JS, Ashley S, Steele D, Ashworth A, Lakhani SR, et al. Basal-like breast carcinomas: clinical outcome and response to chemotherapy. J Clin Pathol. 2006;59:729–35.

4. Lapidot T, Sirard C, Vormoor J, Murdoch B, Hoang T, Caceres-Cortes J, et al. A cell initiating human acute myeloid leukaemia after transplantation into SCID mice. Nature. 1994;367:645–8.

5. Deleyrolle LP, Harding A, Cato K, Siebzehnrubl FA, Rahman M, Azari H, et al. Evidence for label-retaining tumour-initiating cells in human glioblastoma. Brain. 2011;134:1331–43.

6. Dirks PB. Brain tumor stem cells: The cancer stem cell hypothesis writ large. Mol Oncol. 2010;4:420–30.

7. Vermeulen L, de Sousa e Melo F, Richel DJ, Medema JP. The developing cancer stem-cell model: clinical challenges and opportunities. Lancet Oncol. 2012;13:e83–9.

8. Vaillant F, Asselin-Labat M-L, Shackleton M, Forrest NC, Lindeman GJ, Visvader JE. The Mammary Progenitor Marker CD61/β3 Integrin Identifies Cancer Stem Cells in Mouse Models of Mammary Tumorigenesis. Cancer Res. 2008;68:7711–7.

9. Ponti D, Costa A, Zaffaroni N, Pratesi G, Petrangolini G, Coradini D, et al. Isolation and In vitro Propagation of Tumorigenic Breast Cancer Cells with Stem/Progenitor Cell Properties. Cancer Res. 2005;65:5506–11.

10. Collins AT, Berry PA, Hyde C, Stower MJ, Maitland NJ. Prospective Identification of Tumorigenic Prostate Cancer Stem Cells. Cancer Res. 2005;65:10946–51.

11. Patrawala L, Calhoun-Davis T, Schneider-Broussard R, Tang DG. Hierarchical Organization of Prostate Cancer Cells in Xenograft Tumors: The CD44+α2β1+ Cell Population Is Enriched in Tumor-Initiating Cells. Cancer Res. 2007;67:6796–805.

12. Eramo A, Lotti F, Sette G, Pilozzi E, Biffoni M, Di Virgilio A, et al. Identification and expansion of the tumorigenic lung cancer stem cell population. Cell Death Differ. 2007;15:504–14.

13. Beier F, Beier CP, Aschenbrenner I, Hildebrandt GC, Brümmendorf TH, Beier D. Identification of CD133−/Telomeraselow Progenitor Cells in Glioblastoma-Derived Cancer Stem Cell Lines. Cell Mol Neurobiol. 2010;31:337–43.

14. Huang Q, Zhang Q-B, Dong J, Wu Y-Y, Shen Y-T, Zhao Y-D, et al. Glioma stem cells are more aggressive in recurrent tumors with malignant progression than in the primary tumor, and both can be maintained long-term in vitro. BMC Cancer. 2008;8:304.

15. Beck B, Blanpain C. Unravelling cancer stem cell potential. Nat Rev Cancer. 2013;13:727–38.

16. Reya T, Morrison SJ, Clarke MF, Weissman IL. Stem cells, cancer, and cancer stem cells. Nature. 2001;414:105–11.

17. Jordan CT, Guzman ML, Noble M. Cancer Stem Cells. N Engl J Med. 2006;355:1253–61.

18. Sottoriva A, Spiteri I, Shibata D, Curtis C, Tavaré S. Single-molecule genomic data delineate patient-specific tumor profiles and cancer stem cell organization. Cancer Res. 2013;73:41–9.

19. Nakada M, Nakada S, Demuth T, Tran NL, Hoelzinger DB, Berens ME. Molecular targets of glioma invasion. Cell Mol Life Sci. 2007;64:458–78.

20. Galli R, Binda E, Orfanelli U, Cipelletti B, Gritti A, De Vitis S, et al. Isolation and Characterization of Tumorigenic, Stem-like Neural Precursors from Human Glioblastoma. Cancer Res. 2004;64:7011–21.

21. Pollard SM, Yoshikawa K, Clarke ID, Danovi D, Stricker S, Russell R, et al. Glioma Stem Cell Lines Expanded in Adherent Culture Have Tumor-Specific Phenotypes and Are Suitable for Chemical and Genetic Screens. Cell Stem Cell. 2009;4:568–80.

22. Lee J, Kotliarova S, Kotliarov Y, Li A, Su Q, Donin NM, et al. Tumor stem cells derived from glioblastomas cultured in bFGF and EGF more closely mirror the phenotype and genotype of primary tumors than do serum-cultured cell lines. Cancer Cell. 2006;9:391–403.

23. Kleihues P, Sobin LH. World Health Organization classification of tumors. Cancer. 2000;88:2887–2887.

24. Lathia JD, Heddleston JM, Venere M, Rich JN. Deadly Teamwork: Neural Cancer Stem Cells and the Tumor Microenvironment. Cell Stem Cell. 2011;8:482–5.

25. Niclou SP, Danzeisen C, Eikesdal HP, Wiig H, Brons NHC, Poli AMF, et al. A novel eGFP-expressing immunodeficient mouse model to study tumor-host interactions. FASEB J. 2008;22:3120–8.

26. Lathia JD, Gallagher J, Myers JT, Li M, Vasanji A, McLendon RE, et al. Direct In Vivo Evidence for Tumor Propagation by Glioblastoma Cancer Stem Cells. PLoS ONE. 2011;6:e24807.

27. Zeppernick F, Ahmadi R, Campos B, Dictus C, Helmke BM, Becker N, et al. Stem Cell Marker CD133 Affects Clinical Outcome in Glioma Patients. Clin Cancer Res. 2008;14:123–9.

28. Strojnik T, Røsland GV, Sakariassen PO, Kavalar R, Lah T. Neural stem cell markers, nestin and musashi proteins, in the progression of human glioma: correlation of nestin with prognosis of patient survival. Surg Neurol. 2007;68:133–43.

29. Singh SK, Hawkins C, Clarke ID, Squire JA, Bayani J, Hide T, et al. Identification of human brain tumour initiating cells. Nature. 2004;432:396–401.

30. Son MJ, Woolard K, Nam D-H, Lee J, Fine HA. SSEA-1 Is an Enrichment Marker for Tumor-Initiating Cells in Human Glioblastoma. Cell Stem Cell. 2009;4:440–52.

31. Ogden ATMD, Waziri AEMD, Lochhead RA, Fusco D, Lopez K, Ellis JABA, et al. IDENTIFICATION OF A2B5+CD133- TUMOR-INITIATING CELLS IN ADULT HUMAN GLIOMAS. [Miscellaneous Article]. Neurosurg Febr 2008. 2008;62:505–15.

32. Lathia JD, Gallagher J, Heddleston JM, Wang J, Eyler CE, MacSwords J, et al. Integrin Alpha 6 Regulates Glioblastoma Stem Cells. Cell Stem Cell. 2010;6:421–32.

33. Clément V, Dutoit V, Marino D, Dietrich P-Y, Radovanovic I. Limits of CD133 as a marker of glioma self-renewing cells. Int J Cancer. 2009;125:244–8.

34. Hermansen SK, Christensen KG, Jensen SS, Kristensen BW. Inconsistent Immunohistochemical Expression Patterns of Four Different CD133 Antibody Clones in Glioblastoma. J Histochem Cytochem. 2011;59:391–407.

35. Lyons AB. Analysing cell division in vivo and in vitro using flow cytometric measurement of CFSE dye dilution. J Immunol Methods. 2000;243:147–54.

36. Venere M, Fine HA, Dirks PB, Rich JN. Cancer stem cells in gliomas: Identifying and understanding the apex cell in cancer's hierarchy. Glia. 2011;59:1148–54.

37. Nakada M, Nambu E, Furuyama N, Yoshida Y, Takino T, Hayashi Y, et al. Integrin α3 is overexpressed in glioma stem-like cells and promotes invasion. Br J Cancer. 2013;108:2516–24.

38. Zhu X, Morales FC, Agarwal NK, Dogruluk T, Gagea M, Georgescu M-M. Moesin Is a Glioma Progression Marker That Induces Proliferation and Wnt/β-Catenin Pathway Activation via Interaction with CD44. Cancer Res. 2013;73:1142–55.

39. Marhaba R, Zöller M. CD44 in Cancer Progression: Adhesion, Migration and Growth Regulation. J Mol Histol. 2004;35:211–31.

40. Jijiwa M, Demir H, Gupta S, Leung C, Joshi K, Orozco N, et al. CD44v6 regulates growth of brain tumor stem cells partially through the AKT-mediated pathway. PloS One. 2011;6:e24217.

41. Ulrich TA, de Juan Pardo EM, Kumar S. The Mechanical Rigidity of the Extracellular Matrix Regulates the Structure, Motility, and Proliferation of Glioma Cells. Cancer Res. 2009;69:4167–74.

42. Engler AJ, Sen S, Sweeney HL, Discher DE. Matrix Elasticity Directs Stem Cell Lineage Specification. Cell. 2006;126:677–89.

43. Tilghman RW, Cowan CR, Mih JD, Koryakina Y, Gioeli D, Slack-Davis JK, et al. Matrix Rigidity Regulates Cancer Cell Growth and Cellular Phenotype. PLoS ONE. 2010;5:e12905.

44. Georges PC, Janmey PA. Cell type-specific response to growth on soft materials. J Appl Physiol. 2005;98:1547–53.

45. Cheng C-M, Steward Jr. RL, LeDuc PR. Probing cell structure by controlling the mechanical environment with cell–substrate interactions. J Biomech. 2009;42:187–92.

46. Yeung T, Georges PC, Flanagan LA, Marg B, Ortiz M, Funaki M, et al. Effects of substrate stiffness on cell morphology, cytoskeletal structure, and adhesion. Cell Motil Cytoskeleton. 2005;60:24–34.

47. Keung AJ, Kumar S, Schaffer DV. Presentation Counts: Microenvironmental Regulation of Stem Cells by Biophysical and Material Cues. Annu Rev Cell Dev Biol. 2010;26:533–56.

48. Keung AJ, de Juan-Pardo EM, Schaffer DV, Kumar S. Rho GTPases Mediate the Mechanosensitive Lineage Commitment of Neural Stem Cells. STEM CELLS. 2011;29:1886–97.

49. Woolard K, Fine HA. Glioma Stem Cells: Better Flat Than Round. Cell Stem Cell. 2009;4:466–7.

50. Deleyrolle LP, Reynolds BA. Identifying and enumerating neural stem cells: application to aging and cancer. In: Verhaagen EMH, Inge Huitenga, Jan Wijnholds, Arthur B. Bergen, Gerald J. Boer and Dick F. Swaab Joost, editor. Prog Brain Res [Internet]. Elsevier; 2009 [cited 2014 Jun 7]. page 43–51. Available from: http://www.sciencedirect.com/science/article/pii/S0079612309175040

51. Azari H, Millette S, Ansari S, Rahman M, Deleyrolle LP, Reynolds BA. Isolation and expansion of human glioblastoma multiforme tumor cells using the neurosphere assay. J Vis Exp JoVE. 2011;e3633.

52. Reardon DA, Nabors LB, Stupp R, Mikkelsen T. Cilengitide: an integrin-targeting arginine–glycine–aspartic acid peptide with promising activity for glioblastoma multiforme. Expert Opin Investig Drugs. 2008;17:1225–35.

53. Terakawa Y, Agnihotri S, Golbourn B, Nadi M, Sabha N, Smith CA, et al. The role of drebrin in glioma migration and invasion. Exp Cell Res. 2013;319:517–28.

54. Natsume A, Kato T, Kinjo S, Enomoto A, Toda H, Shimato S, et al. Girdin maintains the stemness of glioblastoma stem cells. Oncogene. 2012;31:2715–24.

55. Kobayashi K, Takahashi H, Inoue A, Harada H, Toshimori S, Kobayashi Y, et al. Oct-3/4 promotes migration and invasion of glioblastoma cells. J Cell Biochem. 2012;113:508–17.

56. Alonso MM, Diez-Valle R, Manterola L, Rubio A, Liu D, Cortes-Santiago N, et al. Genetic and Epigenetic Modifications of Sox2 Contribute to the Invasive Phenotype of Malignant Gliomas. PLoS ONE. 2011;6:e26740.

57. Oppel F, Müller N, Schackert G, Hendruschk S, Martin D, Geiger KD, et al. SOX2-RNAi attenuates S-phase entry and induces RhoA-dependent switch to protease-independent amoeboid migration in human glioma cells. Mol Cancer. 2011;10:137.

58. Siebzehnrubl FA, Silver DJ, Tugertimur B, Deleyrolle LP, Siebzehnrubl D, Sarkisian MR, et al. The ZEB1 pathway links glioblastoma initiation, invasion and chemoresistance. EMBO Mol Med. 2013;5:1196–212.

59. Edwards LA, Woolard K, Son MJ, Li A, Lee J, Ene C, et al. Effect of Brain- and Tumor-Derived Connective Tissue Growth Factor on Glioma Invasion. J Natl Cancer Inst. 2011;103:1162–78.

60. Enomoto A, Ping J, Takahashi M. Girdin, a Novel Actin-Binding Protein, and Its Family of Proteins Possess Versatile Functions in the Akt and Wnt Signaling Pathways. Ann N Y Acad Sci. 2006;1086:169–84.

61. Jiang P, Enomoto A, Jijiwa M, Kato T, Hasegawa T, Ishida M, et al. An Actin-Binding Protein Girdin Regulates the Motility of Breast Cancer Cells. Cancer Res. 2008;68:1310–8.

62. Liu J, Tan Y, Zhang H, Zhang Y, Xu P, Chen J, et al. Soft fibrin gels promote selection and growth of tumorigenic cells. Nat Mater. 2012;11:734–41.

63. Beadle C, Assanah MC, Monzo P, Vallee R, Rosenfeld SS, Canoll P. The Role of Myosin II in Glioma Invasion of the Brain. Mol Biol Cell. 2008;19:3357–68.

64. Demuth T, Berens ME. Molecular mechanisms of glioma cell migration and invasion. J Neurooncol. 2004;70:217–28.

65. Sen S, Dong M, Kumar S. Isoform-Specific Contributions of α-Actinin to Glioma Cell Mechanobiology. PLoS ONE. 2009;4:e8427.

66. Sen S, Ng WP, Kumar S. Contributions of talin-1 to glioma cell-matrix tensional homeostasis. J R Soc Interface. 2012;9:1311–7.

67. Levental KR, Yu H, Kass L, Lakins JN, Egeblad M, Erler JT, et al. Matrix Crosslinking Forces Tumor Progression by Enhancing Integrin Signaling. Cell. 2009;139:891–906.

68. Paszek MJ, Zahir N, Johnson KR, Lakins JN, Rozenberg GI, Gefen A, et al. Tensional homeostasis and the malignant phenotype. Cancer Cell. 2005;8:241–54.

69. Samuel MS, Lopez JI, McGhee EJ, Croft DR, Strachan D, Timpson P, et al. Actomyosin-Mediated Cellular Tension Drives Increased Tissue Stiffness and β-Catenin Activation to Induce Epidermal Hyperplasia and Tumor Growth. Cancer Cell. 2011;19:776–91.

70. Sampetrean O, Saga I, Nakanishi M, Sugihara E, Fukaya R, Onishi N, et al. Invasion Precedes Tumor Mass Formation in a Malignant Brain Tumor Model of Genetically Modified Neural Stem Cells. Neoplasia N Y N. 2011;13:784–91.

71. Filatova A, Acker T, Garvalov BK. The cancer stem cell niche(s): The crosstalk between glioma stem cells and their microenvironment. Biochim Biophys Acta BBA - Gen Subj. 2013;1830:2496–508.

72. Coma S, Shimizu A, Klagsbrun M. Hypoxia induces tumor and endothelial cell migration in a semaphorin 3F- and VEGF-dependent manner via transcriptional repression of their common receptor neuropilin 2. Cell Adhes Migr. 2011;5:266–75.

73. Persano L, Rampazzo E, Basso G, Viola G. Glioblastoma cancer stem cells: Role of the microenvironment and therapeutic targeting. Biochem Pharmacol. 2013;85:612–22.

74. Pathak A, Kumar S. Biophysical regulation of tumor cell invasion: moving beyond matrix stiffness. Integr Biol. 2011;3:267–78.

75. Velpula KK, Rehman AA, Chelluboina B, Dasari VR, Gondi CS, Rao JS, et al. Glioma stem cell invasion through regulation of the interconnected ERK, integrin α6 and N-cadherin signaling pathway. Cell Signal. 2012;24:2076–84.

76. Xu Y, Stamenkovic I, Yu Q. CD44 Attenuates Activation of the Hippo Signaling Pathway and Is a Prime Therapeutic Target for Glioblastoma. Cancer Res. 2010;70:2455–64.

77. Torsvik A, Røsland GV, Svendsen A, Molven A, Immervoll H, McCormack E, et al. Spontaneous Malignant Transformation of Human Mesenchymal Stem Cells Reflects Cross-Contamination: Putting the Research Field on Track – Letter. Cancer Res. 2010;70:6393–6.

78. Stepanenko AA, Kavsan VM. Karyotypically distinct U251, U373, and SNB19 glioma cell lines are of the same origin but have different drug treatment sensitivities. Gene. 2014;540:263–5.

79. Piccirillo SGM, Reynolds BA, Zanetti N, Lamorte G, Binda E, Broggi G, et al. Bone morphogenetic proteins inhibit the tumorigenic potential of human brain tumour-initiating cells. Nature. 2006;444:761–5.

80. MacKay JL, Kumar S. Simultaneous and independent tuning of RhoA and Rac1 activity with orthogonally inducible promoters. Integr Biol. 2014;6:885–94.

81. Gallagher PJ, Herring BP, Trafny A, Sowadski J, Stull JT. A molecular mechanism for autoinhibition of myosin light chain kinases. J Biol Chem. 1993;268:26578–82.

82. Ishizaki T, Naito M, Fujisawa K, Maekawa M, Watanabe N, Saito Y, et al. p160ROCK, a Rho-associated coiled-coil forming protein kinase, works downstream of Rho and induces focal adhesions. FEBS Lett. 1997;404:118–24.

83. Shin K-J, Wall EA, Zavzavadjian JR, Santat LA, Liu J, Hwang J-I, et al. A single lentiviral vector platform for microRNA-based conditional RNA interference and coordinated transgene expression. Proc Natl Acad Sci. 2006;103:13759–64.

84. MacKay JL, Keung AJ, Kumar S. A Genetic Strategy for the Dynamic and Graded Control of Cell Mechanics, Motility, and Matrix Remodeling. Biophys J. 2012;102:434–42.

85. MacKay JL, Kumar S. Measuring the Elastic Properties of Living Cells with Atomic Force Microscopy Indentation. In: Taatjes DJ, Roth J, editors. Cell Imaging Tech [Internet]. Humana Press; 2013 [cited 2013 Sep 4]. page 313–29. Available from: http://link.springer.com/protocol/10.1007/978-1-62703-056-4_15

86. Babbin BA, Koch S, Bachar M, Conti M-A, Parkos CA, Adelstein RS, et al. Non-muscle myosin IIA differentially regulates intestinal epithelial cell restitution and matrix invasion. Am J Pathol. 2009;174:436–48.

87. Frey MT, Wang Y. A photo-modulatable material for probing cellular responses to substrate rigidity. Soft Matter. 2009;5:1918–24.

88. Chan CE, Odde DJ. Traction Dynamics of Filopodia on Compliant Substrates. Science. 2008;322:1687–91.

89. Laks DR, Masterman-Smith M, Visnyei K, Angenieux B, Orozco NM, Foran I, et al. Neurosphere Formation Is an Independent Predictor of Clinical Outcome in Malignant Glioma. STEM CELLS. 2009;27:980–7.

90. Ivkovic S, Beadle C, Noticewala S, Massey SC, Swanson KR, Toro LN, et al. Direct inhibition of myosin II effectively blocks glioma invasion in the presence of multiple motogens. Mol Biol Cell. 2012;23:533–42.

91. Kümper S, Marshall CJ. ROCK-Driven Actomyosin Contractility Induces Tissue Stiffness and Tumor Growth. Cancer Cell. 2011;19:695–7.

92. Yu H, Mouw JK, Weaver VM. Forcing form and function: biomechanical regulation of tumor evolution. Trends Cell Biol. 2011;21:47–56.

93. Sen S, Ng WP, Kumar S. Contractility Dominates Adhesive Ligand Density in Regulating Cellular De-adhesion and Retraction Kinetics. Ann Biomed Eng. 2011;39:1163–73.

94. Ruiz-Ontañon P, Orgaz JL, Aldaz B, Elosegui-Artola A, Martino J, Berciano MT, et al. Cellular Plasticity Confers Migratory and Invasive Advantages to a Population of

Glioblastoma-initiating Cells that Infiltrate Peritumoral Tissue. STEM CELLS. 2013;N/A – N/A.

95. Reyes SB, Narayanan AS, Lee HS, Tchaicha JH, Aldape KD, Lang FF, et al. αvβ8 integrin interacts with RhoGDI1 to regulate Rac1 and Cdc42 activation and drive glioblastoma cell invasion. Mol Biol Cell. 2013;24:474–82.

96. Hirata E, Yukinaga H, Kamioka Y, Arakawa Y, Miyamoto S, Okada T, et al. In vivo fluorescence resonance energy transfer imaging reveals differential activation of Rho-family GTPases in glioblastoma cell invasion. J Cell Sci. 2012;125:858–68.

97. Shin J-W, Buxboim A, Spinler KR, Swift J, Christian DA, Hunter CA, et al. Contractile Forces Sustain and Polarize Hematopoiesis from Stem and Progenitor Cells. Cell Stem Cell. 2014;14:81–93.

98. Lathia JD, Li M, Hall PE, Gallagher J, Hale JS, Wu Q, et al. Laminin alpha 2 enables glioblastoma stem cell growth. Ann Neurol. 2012;72:766–78.

99. Wong SY, Ulrich TA, Deleyrolle LP, MacKay JL, Lin J-MG, Martuscello RT, et al. Constitutive Activation of Myosin-Dependent Contractility Sensitizes Glioma Tumor-Initiating Cells to Mechanical Inputs and Reduces Tissue Invasion. Cancer Res. 2015;75:1113–22.

100. Asokan A, Schaffer DV, Samulski RJ. The AAV vector toolkit: poised at the clinical crossroads. Mol Ther J Am Soc Gene Ther. 2012;20:699–708.

101. Berns KI, Linden RM. The cryptic life style of adeno-associated virus. BioEssays News Rev Mol Cell Dev Biol. 1995;17:237–45.

102. Huttner NA, Girod A, Perabo L, Edbauer D, Kleinschmidt JA, Büning H, et al. Genetic modifications of the adeno-associated virus type 2 capsid reduce the affinity and the neutralizing effects of human serum antibodies. Gene Ther. 2003;10:2139–47.